Centre for Geo-Information

Thesis Report GIRS-2015-01

Improving forest monitoring:

(Combining temporal and spatial information to enable for an automated and accurate detection of forest cover change)

Amalia Castro Gómez

12 January 2015

WAGENINGEN UNIVERSITY
WAGENINGEN UR

Improving forest monitoring:

Combining temporal and spatial information to enable for an automated and accurate detection of forest cover change

Amalia Castro Gómez

Registration number 89 12 12 156 120

Supervisors:

phD Eliakim Hamunyela
dr. ir Jan Verbesselt

A thesis submitted in partial fulfilment of the degree of Master of Science
at Wageningen University and Research Centre,
The Netherlands.

12 January 2015
Wageningen, The Netherlands

Thesis code number: GRS-80436
Thesis Report: GIRS-2015-01
Wageningen University and Research Centre
Laboratory of Geo-Information Science and Remote Sensing

ACKNOWLEDGEMENTS

I would like to thank all the people who contributed in some way to the work described in this thesis. First and foremost, I would like to express my sincere gratitude to my main supervisor phD Eliakim Hamunyela for his patient guidance, his dedication and his knowledge. I have been extremely lucky to have a supervisor who cared so much about my work and who was always available to help, making such an effort to give detailed feedback and to answer my queries promptly. I greatly benefited from his keen scientific insight and his ability to simplify complex ideas, and would not have been able to improve so much without his expert guidance.

I would also like to express my deep appreciation and gratitude to my supervisor dr. ir. Jan Verbesselt, for his patient mentorship and guidance, all the way from the initial stage of selecting a thesis topic to the completion of this work. His expertise and his kindness have been an essential support through the different challenges I encountered and I consider myself fortunate to have had the opportunity to work with him.

I would also like to thank all the members of the Laboratory of Remote Sensing who helped me in the process and who supported me during this thesis. In particular I would like to thank Prof. dr. Martin Herold and dr. ir. Jan Clevers for the detailed feedback they provided on the thesis proposal, as well as phD Loic Dutrieux for his advice in reference to chapter 4(sections 4 and 6). I wish as well to thank ing. Willy Ten Haaf for his kindness and support throughout the thesis.

Finally I must express my gratitude as well to my fellow students for their advice, feedback, and friendship, and to my parents, brothers and boyfriend for their patience, encouragement and unconditional support.

INDEX

ABSTRACT

In the context of REDD+, the accurate identification of active forest change areas from remote sensing sensors is essential to monitor, report and verify tropical deforestation efficiently. Landsat imagery is considered the most viable option due to its high-resolution data, and extensive and free archive. However, the high level of noise (e.g. clouds or climatic disturbances) in Landsat data from tropical areas reduces the reliability of the detection of deforestation. Pre-processing is essential in order to detect deforestation reliably, but for Landsat no comprehensive methodology for cloud screening is available, and the correction of external disturbances remains to be addressed. The main objective is to improve the detection of deforestation from Landsat image time series by including information of the spatial neighbourhood of a pixel. First the preprocessing is enhanced by distinguishing between outliers and potential change events with a temporal threshold. Next, the information present in the spatial context of a pixel is used to correct for the influence of external disturbances. The detection of deforestation is based on the corrected time series and uses the Break detection For Additive Season and Trend Monitor (BFASTmonitor) method. A series of experiments are described that have two different objectives: (i) define the optimal value of the temporal threshold that removes remnant outliers and test its influence on the detection of deforestation, (ii) optimize the selection of neighbouring pixels whose spectral information is used to correct for external disturbances. The influence of each test on the detection of is determined and the approach that allows for the most accurate detection is chosen. Outliers could be distinguished from deforestation events with a temporal threshold shorter than a year (104 days) but the detection was only slightly improved. In fact, before removing remnant outliers, the overall accuracy was 87%, and the commission and omission errors were 8.5% and 4.5%, and after the removal the corresponding values were 87.25%, 7% and 5.75%. The spatial neighborhood information could not be used to correct effectively for the effect of external disturbances, notably during the monitoring period, due to the high level of noise present in the data. The overall accuracy was lowered to 59.68% and the commission and omission errors rose to 17.74% and 22.58%. Results highlight that the combination of Landsat data with techniques that correct for external disturbances using the spatial context of a pixel remains complicated due to the irregularity of the data and to cloud contamination. Further efforts are needed to develop and optimize approaches that reduce the noise from Landsat and Landsat-derived time series in tropical areas.

Keywords: Landsat, tropic, deforestation, monitoring, spatial, temporal, disturbance

List of Figures

1- Introduction

Carbon dioxide (CO_2) is the most important greenhouse gas (Hyman et al., 2002), and its concentration in the atmosphere continues to increase, hence accelerating global warming (Cox et al., 2000). Forest cover change through deforestation is one of the major contributors to atmospheric CO_2 (Gibbs et al., 2007; Houghton, 1991; House et al., 2002). With the aim to reduce the rates of deforestation and forest degradation processes, the United Nations Framework Convention on Climate Change (UNFCCC) proposed a mechanism known as Reducing Emissions from Deforestation and Forest Degradation (REDD+) whereby developing countries are compensated monetary for keeping their forests intact for specified period of time (Holloway & Giandomenico, 2009; Phelps et al., 2010; Román-cuesta, 2010). REDD+ uses a definition of deforestation that relies on thresholds related to the area affected, to vegetation height and to tree canopy cover. Any area that is considered as deforested has to extend over a minimum of 0.05-1ha, have a tree canopy cover between 10 and 30% and a maximum tree height of 5m (Herold & Johns, 2007). In other terms, deforestation is the conversion of forest to another land-cover type (Herold & Skutsch 2011).

Understanding the impact of deforestation and regrowth processes in carbon dynamics requires an accurate account of carbon stocks. Therefore it needs a quantification of forest biomass variability as well as an extensive mapping of forest disturbances and regrowth over time. Hence, the data collected for this purpose must cover large areas and be recorded over long periods of time. The use of remote sensing techniques from satellite platforms presents various advantages in this regard when compared to approaches based on inventories. While inventories rely on sampling, and are therefore limited by the frequency and distribution of the samples (Powell et al. 2010), remote sensing techniques can provide frequent information on state of forest over large areas. In addition to that, remote sensing techniques can give a deeper understanding on forest dynamics. It is possible to derive indicators of ecosystem dynamics and to analyse their temporal behaviour, both from a historic perspective and in near-real time, while accounting for seasonal ecosystem variation. As a result, early alerts of crucial changes can be produced in an accurate and cost effective way (Verbesselt et al., 2012). In the context of REDD+, remote sensing is a key observation tool that includes mainly optical data, but also thermal, Synthetic Aperture Radar (SAR) and Light Detection

And Ranging (LiDAR) data. Time series derived from remote sensing can be used to fill historic monitoring gaps and to compare historical and expected forest changes to the desired state. As a result, remote sensing data are combined with ground measurements to estimate and monitor changes in the area affected by deforestation or degradation and changes in the density of carbon stock. The final objective is to measure, report and verify forest carbon emissions in an objective, practical and cost-effective way (De Sy et al. 2012).

Implementing REDD+ in an effective way translates into ensuring fast responses or interventions to forest changes. This relies on the identification of active forest change areas (hotspots), and near-real time detection is central in this regard (De Sy et al. 2012). Monitoring and verifying tropical deforestation in an efficient way depends on two aspects: (i) a sufficiently high spatial resolution and (ii) the temporal density of observations (DeFries et al. 2005). This last aspect translates into a sufficient temporal resolution and into the capacity to observe surface through the atmosphere, where clouds represent the main obstacle for an accurate observation (Asner, 2001).

Clouds produce abnormally low NDVI values that reduce the data quality (Bradley et al., 2007). The accuracy of the detection of abrupt and climatic changes, which depends on the magnitude of the change versus the signal-to-noise ratio is then affected (Verbesselt et al., 2010; Verbesselt et al. 2012). However, the usefulness of remote sensing data from the different sensors available for tropical forest monitoring is limited. On one hand optical sensors are affected by recurrent cloudiness and on the other hand there is a lack of consistent, continuous and affordable coverage from sensors that are not affected by cloudiness (e.g. SAR or LiDAR data). This is partly due the lack of useful optical data when cloudiness is recurrent over the area, and to the lack of consistent, continuous and affordable coverage from standard fine resolution data or from SAR and LiDAR data, which are not affected by cloudiness (De Sy et al. 2012). Using different sensors in a synergic way, to benefit from their different spectral, spatial and temporal characteristics, offers a solution for limitations in data availability (cloudiness and limited temporal and spatial coverage of a certain area) (De Sy et al. 2012; Goetz et al. 2009). Coarse resolution optical sensors (e.g. the Moderate Resolution Imaging Spectroradiometer, MODIS) acquire frequent observations over large areas. They are therefore useful in overcoming issues with data gaps due to cloud cover (Morton et al. 2006) but not to identify small scale deforestation patches (Achard et al. 2007; Jin and Sader 2005; Olander et al. 2008; Verbesselt et al., 2010). However, coarse

resolution optical sensors can be useful to locate hotspots of forest area changes that can later on be analysed with finer spatial resolution data (De Sy et al. 2012). Optical medium resolution sensors such as Landsat measure with a finer spatial resolution, which is particularly suitable for monitoring small scale changes (Morton et al. 2006; DeFries et al. 2005). Furthermore, using Landsat images from current and previous missions allows users to obtain a detailed dense and extensive historical record of forest dynamics (Kennedy et al. 2010). However, the minimum revisiting time of Landsat (each 16 days) is often extended because of cloud contamination (Hilker et al. 2009), which is a main issue for data interpretation in tropical areas (Olander et al. 2008; Herold & Johns 2007, Asner 2001).

For near real-time detection of deforestation, the fusion of coarse spatial resolution data, which have a high temporal resolution, with moderate spatial and temporal resolution data offers great possibilities. They allow to identify areas of rapid change that can later on be analysed in detail with finer spatial resolution data, and to develop a warning system. It has been proposed for example to use a combination of Landsat time- series data and MODIS imagery to overcome issues with MODIS products (different images of the same area have varying pixel size, viewing angle and area of coverage). Therefore Xin et al (2013) suggested a method to use Landsat time-series to predict the value of a future MODIS image. In this way, which assumes that no disturbance has occurred before the future MODIS image is recorded, it is possible to compare the predicted expected value with the real recording. If there is a difference between both spectral signatures, this difference is used to represent the change. However, in general terms, fusion techniques need to be further developed, tested and evaluated (De Sy et al. 2012). Even though using a single satellite sensor instead of a fusion of several generally limits the advantages from combining spatial, spectral and temporal resolutions (Xin et al. 2013), as long as the products derived are useful, using single sources is considered the best choice due to its simplicity (De Sy et al. 2012). Landsat imagery offers an optimal combination of high resolution data, extensive archive and freely accessible data, and is therefore the most viable option when monitoring deforestation in the context of REDD+ (Olander et al. 2008; Defries et al. 2007; Herold & Johns 2007).

Many approaches have been proposed to detect changes using Landsat time series (e.g. LandTrendr (Kennedy et al. 2007), Vegetation Change Tracker (Huang et al. 2010) or curve fitting algorithms (Powell et al. 2010)) but are not adapted for near-real time purposes. Near real-time change detection algorithms must be capable of distinguishing the normal

phenological cycle from abnormal behaviour in newly acquired satellite data (Verbesselt et al. 2012). Several near-real time detection approaches have been developed using MODIS imagery (Jiang et al. 2010; Verbesselt et al. 2012; Verdin et al. 2005; White & Nemani, 2006) and could potentially be used with Landsat products. Among those, the BFASTmonitor approach optimizes detection because it uses the full temporal detail of the time series, does not depend on user-defined vegetation-specific thresholds and can deal with missing data in an effective way (Verbesselt et al. 2012). It is an extension of the Break Detection For Additive Season and Trend season-trend model (BFAST), which detects and characterizes changes only in historic time-series (Verbesselt et al. 2010). Instead, BFASTmonitor allows for the detection and characterization of the change in near-real time by first analysing the historic time-series and identifying a stable part of the historic time-series. Next, it adjusts a season-trend model to this stable period, representing the expected variation of the data. Finally it assesses if the model remains stable for incoming data, and hence is able to signal a break if their variation differs from the expected one (Verbesselt et al. 2012).

2- Problem definition

Deforestation in the tropics is responsible for most of the global net carbon flux derived from land use changes (Achard et al. 2007). The importance of monitoring it in near-real time to enable early warnings and responses has been widely acknowledged in the scientific community (Morton et al. 2006; Verbesselt et al. 2012). However, a comprehensive approach to monitor globally and in near-real time forest disturbances including small scale human activities is lacking (Xin et al. 2013). This is due to various specific reasons. In the following part the different reasons are reviewed in detail together with the current state of the art of methodologies that address them.

2-1- The problem of cloud removal in change detection with Landsat data:

The benefits of using enhanced quality data where clouds have been removed when applying methods for change detection has been acknowledged (Verbesselt et al. 2010). However, cloud coverage and cloud shadow currently remains one of the main challenges when correcting signal contamination in tropical areas that are often cloudy (Gibbs et al. 2007;

Hagolle et al. 2010; Townshend & Justice, 2002), and clouds and cloud shadows need to be precisely identified and removed to enable for an automated time series analysis (Zhu & Woodcock, 2012).

Several approaches have been developed for cloud screening in data from coarse resolution sensors, and are therefore not specific to Landsat. They depend on the spectral bands available on the specific sensor, and on the characteristics of each type of cloud. For example, they use visible and thermal infrared bands to locate clouds because clouds are colder than the surface and are in this case applied to MODIS or Advanced Very High Resolution Radiometer (AVHRR) data (Ackerman et al. 1998; Saunders & Kriebel, 1988), or short wave infrared (SWIR) bands to detect high clouds in Airborne Visible/Infrared Imaging Spectrometer (AVIRIS) data (Gao et al. 1993). The neighbouring information is also used to discriminate clouds (Ackerman et al. 1998; Saunders & Kriebel, 1988). Other algorithms rely on multi-temporal observations to detect clouds, but they are not common and follow different approaches. For instance, they look for low correlation between successive images (Lyapustin et al. 2008), or rely on daily temperature observations to analyse the smooth variations and classify outliers as clouds (Reuter et al. 2005).

Current cloud screening methods for Landsat imagery are very heterogeneous and follow different approaches. It is possible to use classification methods in each acquired scene (Hansen et al. 2008; Kennedy et al. 2007; Sano et al. 2007) as well integrated segmentation and object based classification (Goodwin et al. 2013). Another possibility is to use single-date Landsat imagery cloud/shadow screening approaches that rely on spectral filters, to distinguish clouds and cloud shadows from surfaces with similar spectral signatures (Goodwin et al., 2013). One of those approaches has been used traditionally to remove clouds from Landsat scenes, and is referred to as Automatic Cloud Cover Assessment (ACCA) algorithms (Irish et al. 2006; Choi & Bindschadler, 2004; Roy et al. 2010) but is not sufficiently precise for time series analysis regarding the location and boundaries of clouds and cloud shadows. Other single-date screening algorithms are based on MODIS algorithm (Oreopoulos et al. 2011). They are implemented as the Landsat Ecosystem Disturbance Adaptive Processing System (LEDAPS) for geometric and radiometric correction, and have been adapted from the MODIS Adaptive Processing System (MODAPS) (Masek et al. 2006; Feng et al. 2012; Justice et al. 2002). LEDAPS enables users to rapidly produce surface

reflectance products from raw radiometry for a large amount of Landsat images (Feng et al. 2012) but may nevertheless not detect clouds accurately when the area is largely covered by them (Zhu & Woodcock 2012). Finally the Function of mask (Fmask) approach uses a probability mask and a scene-based threshold for the classification of pixels contaminated by clouds (Zhu & Woodcock 2012). Fmask is successful in classifying clouds and cloud shadows as such (high producer accuracy). Despite the fact that thin warm clouds may not be detected (omission errors), it is still possible to remove them with atmospheric correction. The main limitation for Fmask results from the fact that it applies a scene-based threshold to all pixels, and therefore its results may not be good enough in scenes with complex surface reflectance (Zhu & Woodcock 2012).

There is no comprehensive set of algorithms available for cloud detection in Landsat imagery (Hagolle et al. 2010; Zhu & Woodcock, 2012). Despite using high resolution data and the recent improvements in high-level preprocessing techniques, cloud detection methods need to be further optimized (Hagolle et al. 2010; Tucker & Townshend, 2000, Michishita et al. 2014). When analysing time series, it is possible to use the temporal context of an observation. This is based on the assumption that a change in the vegetation due to deforestation shows a recognizable abrupt drop of the NDVI value and is followed by a gradual increase over time (regrowth). The concept is in fact a simple adaptation of the approach proposed by Viovy et al. (1992) known as the best index slope extraction (BISE) filter. The concept relies therefore on the fact that a drop due to a change in vegetation will be distinct from the high-frequency change derived from cloud conditions, where the sharp decrease in vegetation index value is immediately followed by an increase.

2-2- The effect of external disturbances

Some challenges still remain to improve the detection of deforestation with methods designed to work in near real time. The importance of pre-processing methods to enhance the quality of the data and the reliability of the detection with BFASTmonitor has been acknowledged (Verbesselt et al. 2012). Reducing noise in the time series involves screening effectively cloud cover and cloud shadows, but other external disturbances affect as well the data quality. The external disturbances can include seasonal or phenological effects, errors in the radiometric or atmospheric correction, topographic impacts or effects of the bidirectional reflectance distribution function (Lhermitte et al. 2011) as well as human-induced or climatic

disturbances (Nelson, 1994). For example, drought is likely to be the main natural factor affecting ecosystems productivity in the context of climate change (Malhi et al. 2009). Correcting for the effect of external disturbances in the time series is challenging, because the change observed in a certain area can be due to natural climatic variations, to anthropogenic disturbance, or to a combination of both (Coppin et al. 2004). The spectral properties of the disturbance are of particular importance (Schroeder et al. 2011), and it is possible to improve further the detection of changes by including spectral information present in the spatial context of a given area. Some approaches have been proposed in literature that can correct for the effect of external disturbances and phenological variations in a certain patch by including the spectral information of neighbouring areas. In the case of the Regeneration Index (RI) approach (Diaz-Delgado et al. 1998), the correction relies on the selection of neighbouring control plots, unaffected by the studied change, that describe the vegetation behaviour in the case that no change had occurred (Lhermitte et al. 2010). However the approach depends on static reference data, which are not always available or have a coarse scale. Furthermore, the method cannot consider heterogeneity within each studied area (Lhermitte et al. 2010). This approach was adapted by Lhermitte et al. (2010) to correct for those disadvantages, in an index referred to as pixel-based Regeneration Index (pRI). The pRI can quantify vegetation dynamics separately for each pixel within an affected area, by incorporating information of control pixels. The control pixels are selected based on the similarity of their time series and on the spatial context (Lhermitte et al. 2011). The pRI has traditionally been applied for fire assessment purposes, with different indices derived from MODIS, Landsat and SPOT (Lhermitte et al. 2011; Veraverbeke et al. 2010, 2011, 2012). The pRI is acknowledged to be a valuable tool to represent intra-annual variations when data from moderate to coarse spatial resolution are used (e.g. from SPOT or MODIS). Landsat products have been used in bi-temporal estimates of fire impact on vegetation over non-tropical areas (Lhermitte et al. 2011). The correction of external disturbances with the pRI based on irregular Landsat products with a high amount of missing data (tropical areas), and on a monitoring approach robust to data gaps such as BFASTmonitor remains to be assessed.

2-3.Research objectives and research questions

The main objective of this study was to improve the detection of deforestation from Landsat image time series. First, we tested an approach to remove remnant outliers from NDVI Landsat time series and evaluated its performance with BFASTmonitor. We then assessed

Fig. 1. Location of the study area (red) in the northern part of Brazil, state of Pará.

whether combining BFASTmonitor with an analysis of the spectral and spatial properties of the detected disturbance improved further the accuracy of the BFASTmonitor results.

The research questions this study aimed to answer were:

1. Can we distinguish temporally outliers from a deforestation event in our area?
2. Can remaining outliers robustly be removed from Landsat image time series, to improve Landsat-based deforestation monitoring?
3. Can spatial neighbourhood information be used correct for the influence of external disturbances?

3- Materials

3-1. Study area

The study area is located in the northeast area of the region of Pará, in the north of Brazil. The area, which can be located with Fig. 1, is limited by the coordinates -48° 15' 49.5" and -48° 7' 25.9674" in longitude and -2° 53' 33.6192" and -2° 42' 11.8224" in latitude. The site covers an area of 325 710 km^2 (21 km x 15.5 km). The forest in the region of Pará is evergreen (Uhl & Vieira, 1989) and the climate is humid tropical, with an annual rainfall average of 2200 mm. The dry season usually takes place from July to November (Asner et al., 2001), with generally less than 50 mm per month (Pereira et al., 2002). Often June and December are dry enough to allow logging operations (Pereira et al., 2002). The area has soils classified as argisols and the topography is flat to mildly undulating (Asner et al., 2001).

This site is particularly interesting for our study because it is located in the tropics and it is among the states with higher deforestation rates (together with the states of Mato Grosso, Maranhao and Roraima (UNEP-GEAS, 2010). Pará has been subjected to heavy logging activities from the end of the 1960s, because the Belém-Brazilia highway enabled easy access to the region. The land was sold for low prices, resulting in an expansion of cattle ranches that transformed large areas of forest into pasture (Uhl & Vieira, 1989). However ranching gradually decayed due to economic and ecological constraints, and timber exploitation activities developed strongly (Uhl & Vieira, 1989). In the last years, the financial support from the Brazilian government to soybean agriculture notably increased the extent of cultivated areas in the Paragominas region (Souza et al. 2009). Deforestation is therefore mainly due to commercial logging and to conversion of forest land to agriculture (WWF, 2013). For commercial logging, trees are cut and sold as timber or pulp. It can occur selectively (i.e. selective logging), where only the valuable species are cut, or by clear-cutting, where all the trees in the area are removed (Tropical Rain Forest Information Center, 1998). Both logging procedures use heavy machinery to remove trees and build roads, which is a major cause of disturbance (Tropical Rain Forest Information Center, 1998). When the area is deforested for agricultural purposes, the deforestation procedure usually involves slashing and burning the area. Small landholders of the state of Pará practiced slash and burn extensively in the past, and therefore this practice occurs generally over smaller areas than modern intensive agriculture (Rodrigues et al, 2003). The trends seem to indicate a general decrease in the rate of deforestation for this state, even though the years of 2012 and 2013 registered a general increase (UNEP-GEAS, 2010; WWF, 2013).

3.2. Data

Vegetation dynamics were analysed from the NDVI product of Landsat 4-5 TM and Landsat ETM+ geo-referenced imagery (with ground control points), covering the period from 1987 to 2014. These scenes belong to path/row 223/062 and have a spatial resolution of 30m and were sourced from the Earth Explorer site of USGS (www.earthexplorer.usgs.gov).

Areas that had remained as forest until the start of the monitoring period were identified using the Landsat Vegetation Continuous Field dataset of year 2000 (VCF) and the Landsat Forest Cover Change (FCC). Both datasets are Landsat-based products and have a spatial resolution of 30m (GLCF-GSFC, 2014). They were obtained from the Global Land Cover

Facility site (www.landcover.org). The VCF dataset estimates the percentage of horizontal ground in each pixel that is covered by woody vegetation of a height of 5m or more (Sexton et al. 2013). The FCC dataset is based on the VCF products and identifies the changes in forest cover between the years 2000 and 2005 with a certain probability per pixel. It enabled us to locate the pixels that had remained as forest up year 2005 included. This study does not aim to evaluate and improve the temporal delay of the detection of deforestation with BFASTmonitor. Instead, it is focused on improving the spatial accuracy. Therefore, the monitoring was not performed in near-real time. FCC data extend up to year 2005, hence the start of the monitoring period was fixed and corresponded to year 2006. The F-mask layer available for each Landsat scene in the corresponding Surface Reflectance product was used to remove clouds as much as possible.

Rainfall data from Tropical Rainfall Measuring Mission (TRMM) of NASA, of Level 3 (3B43) were used to calculate standard precipitation index (SPI) in order to estimate the occurrence of drought in the area (McKee, et al. 1993). TRMM data are recorded monthly from 1998 to 2013, and are available for free download from the website of the NASA-Goddard Earth Sciences Data and information services Centre (http://disc.sci.gsfc.nasa.gov). For validation, the study used True Colour composites created using the Surface Reflectance product (bands 1, 2 and 3). The statistical analysis of time-series, the pre- and postprocessing of Landsat imagery and the validation were performed in the opensource R software for statistical computing (version 3.0.2) (R Development Core Team, 2011), where the BFASTmonitor function is developed within the *bfast* package.

3.3. Selection of forested pixels

To select only the pixels that had remained forest during the historic period, it was taken into account that REDD+ considers an area as forest if 30% or more of its extent is covered by trees (Herold & Johns, 2007). It was possible to select pixels that fulfil this criterion using VCF layer of year 2000., by selecting only the pixels with a percentage of woody vegetation equal or higher to 30%. Next, the FCC layer was used to further select those pixels that were classified as Persistent Forest between the years of 2000 and 2005 with a probability of 90%. Fig. 2 presents the forested pixels analysed in this study, overlaid over a true colour composite of a Landsat acquisition of the study area.

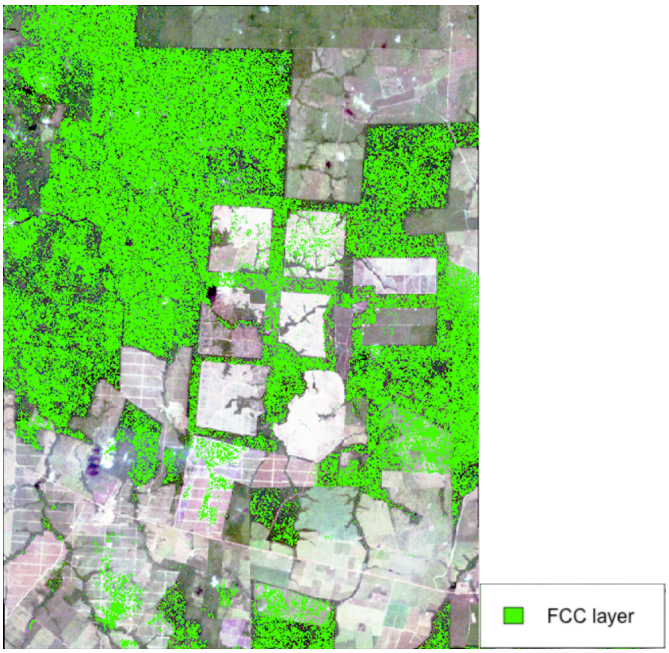

Fig. 2 Pixels considered as forest at the start of the monitoring period in year 2006 (in light green). This selection of pixels is based on the VCF layer of year 2000 and on the FCC layer of years 2000-2005. The final pixels selected for the study has at least 30% of woody vegetation cover by year 200. Furthermore, they remained as forest between years 2000 and 2005 with a probability of at least 90%. The background shows a true-colour Landsat acquisition of the study area

4-Methods

An overview of the study methodology is shown in Fig. 3. The first analysis tests if removing remnant outliers (mostly clouds) improves the accuracy of the detection of deforestation with BFASTmonitor, compared to the BFASTmonitor result where remnant outliers have not been removed (sections 4.1 and 4.2.). After this, the most accurate dataset is chosen, and we seek to further improve the detection with a spatial analysis. Therefore the second analysis tests if including information of the neighbouring area of a certain pixel can optimize the detection. The result of this step is compared with the previous results. Finally, the most accurate BFASTmonitor is chosen.

4.1- Preliminary analysis: Adjusting the temporal threshold approach

Outliers can result from a variety of causes, such as atmospheric influences, sensor performance, or the efficiency of post-acquisition cloud algorithms (Geerken, 2009). The

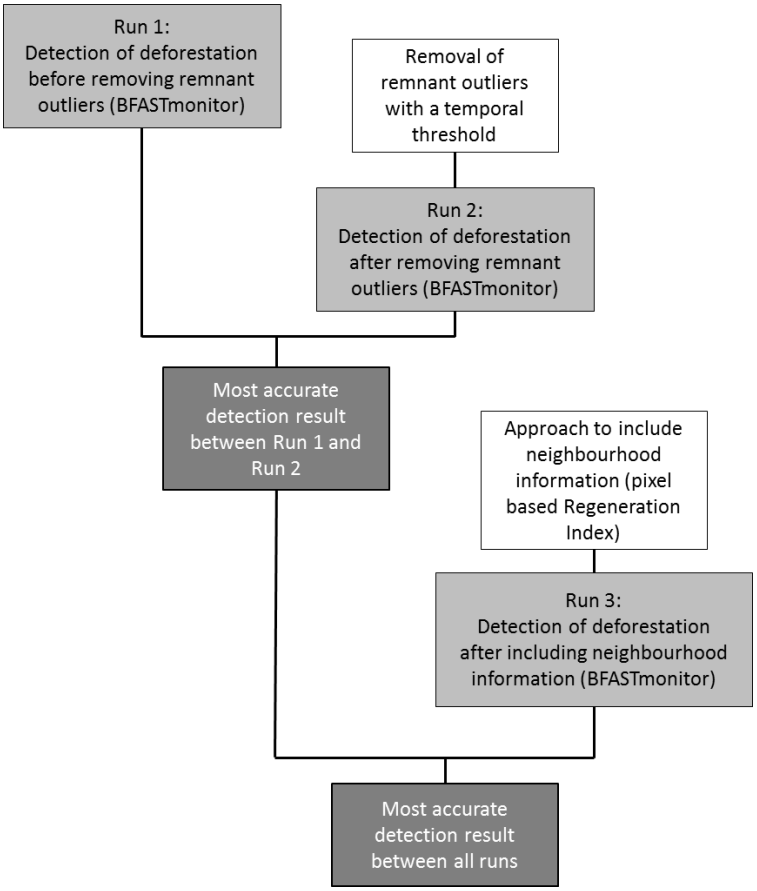

Fig. 3 Overview of the study methodology. The accuracy of the detection of deforestation with BFASTmonitor is tested before (Run 1) and after (Run 2) an approach that aims to remove remnant outliers. The most accurate change detection procedure of both cases is selected. Then an additional procedure is tested, that builds upon the previously selected one (Run 1 or Run 2). This additional procedure includes information of the spatial context of a pixel (Run 3). Finally the most accurate approach is selected.

objective of the preliminary analysis was to define a temporal threshold that could differentiate clearly the drop in NDVI caused by an outlier (e.g. cloud) from that of deforestation. First, three test values for the temporal threshold were defined based on a literature review. The values were then tested, and the one that produced more accurate results was chosen. There is evidence in literature that the scientific community does not have an integrated view of the recovery processes of forests, and that detailed long-term studies are needed to achieve a complete understanding (Chazdon, 2003). The factors influencing recovery are directly and indirectly linked to the ability of the affected area to sprout or resprout, where the type of deforestation plays a major role (e.g. in the presence of burning practices , the recovery will be slower). Literature indicates that the identification of a clear

response to a certain disturbance in temporal behaviour of vegetation may not be possible, because recovery processes following different kinds of disturbances (natural or anthropogenic) overlap both in space and in time (Chazdon 2003). Furthermore, the recovery process can present an important spatial heterogeneity (Chazdon, 2003). Characterizing recovery processes is very complex and was out of the scope of this study. It is possible however to make some relative and quantitative estimations. As stated previously, logging (selective or clear-cutting) and slash and burn are the main deforestation activities occurring in the region of Pará. Selective logging and clear-cutting may present faster rates of recovery than areas where slash and burn practices occurred, however the size of the area affected could play an important role. Furthermore, forest areas in the study have low land-use intensity in the historic period because they are assumed to have remained as forest. Also, remnant forests are found nearby, which can shorten recovery through seed dispersion. Therefore disturbed patches in our area are expected to present relatively accelerated recovery rates. It is difficult to derive quantitative measures for the recovery because studies measuring recovery are rare in the scientific literature, but some of them can be found related to the recovery after logging in other tropical areas, and can be useful for our purpose. In Indonesia, one year after logging the density of trees was of 41% of the previous levels (Cannon, 1998). In Brazil, in the Tapajos National Forest, growth increased only the first 3 years after logging (Chazdon, 2003). Finally, in Malaysia, one year after logging the area contained biomass between 44 and 67% of the pre-logging levels (Pinard et al. 1996). Based on these studies, a temporal threshold of less than one year was considered as suitable for the distinction of outliers from deforestation events in the NDVI time series. Different temporal threshold values were selected for testing, to assess their effect on the accuracy of BFASTmonitor. Finally the most appropriate temporal threshold value was chosen for the further steps.

4.2- Removing remnant outliers

The objective of the next step of this study was to remove the outliers that previous pre-processing techniques (Fmask) could not remove, i.e. remnant outliers. This is important because, as discussed previously, traditional cloud algorithms such as Fmask may have a limited success removing clouds and therefore not taking this into account can affect negatively the accuracy of change detection. Hence the goal was to determine whether additional outlier removal techniques can improve detection of the deforestation. We

corrected the outlier values with a temporal threshold approach that aimed to be conservative. This approach determined whether the period measured from the moment the NDVI value dropped under the median until the moment it recovered could correspond to a deforestation event, or if on the contrary it was too short to be plausible and corresponded instead to an outlier.

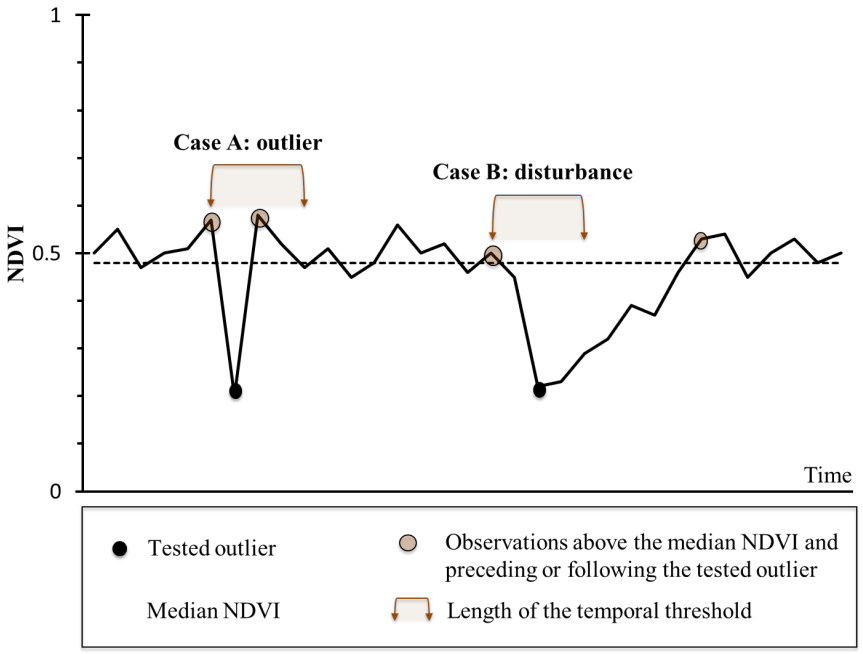

Fig. 4 Illustration of the concept applied to remove remnant outliers from NDVI time series with the temporal threshold approach. The observations with an NDVI value lower than that of the median NDVI of the time series are considered as potential remnant outliers, and tested with the temporal threshold approach. The temporal threshold represents a certain length of time, that discriminates potential disturbance cases from outliers as follows. First the length of time between the observations immediately preceding and following a potential outlier are identified. Next, the time span between such observations is measured, and compared to the temporal threshold. Measured time spans shorter than the temporal threshold are considered unrealistic, and therefore the outlier observation was discarded.

4.3-Applying BFASTmonitor to NDVI time series

BFASTmonitor detects disturbances in the time series, from a date that separates historic and monitoring period. Therefore, disturbances are detected by comparing the variation of the data in the monitoring period with the variation of the data in a stable historic period. The

comparison involves identifying a stable part of the historic period, and modelling its variation. This model represents the normal dynamics for the historic period in the area, i.e. the variation that is expected in the monitoring period. The model has certain unknown parameters, which are the intercept, the slope, the amplitudes and the phases, and which are estimated based on the stable historic period. The model fitted is robust against gaps in the time series because the missing observations are not considered for the estimation of the unknown model parameters (Verbesselt et al. 2012). If this model does not remain stable for the incoming observations in the monitoring period, i.e. if there is an abnormal variation, then a disturbance is detected.

It is very important to select a stable historic period free of disturbances, to ensure that the model fitted represents accurately the normal expected behaviour of vegetation. Different approaches are available for this selection, and in order to choose the best adaptation of the BFASTmonitor model the characteristics of the area and of the data were considered. The typical interval between Landsat acquisitions is not regular, and the presence of outliers (mainly due to clouds) varies from pixel to pixel. This results in time series composed of relatively sparse sections, and which are furthermore likely to contain outliers even after the step of removing the remnant ones. To ensure that the pixels analysed contained sufficient data and that would therefore not fit the BFASTmonitor model based on a few observations, the pixels that presented less than 80 observations in the historic period and less than 44 in the monitoring period after the removal of remnant outliers were masked out, and were therefore not used for the validation of the temporal threshold approach nor for the spatial context analysis. Appendix 1 shows the amount of observations per pixel in the study area.

Seasonality in the data is assumed to be marginal because the forest type is evergreen (Reiche et al. 2015). It is reasonably safe to assume that the pixels analysed remained as forest in the history period. However climatic disturbances may have taken place in the historic period, and can also produce a pattern in the model fitted to the historic period, with an increasing or decreasing trend (decreasing is the more likely due to drought). Including the trend component in the model would lead to inaccurate predictions of the values in the monitoring period, i.e. wrong detections. For these reason we omitted the seasonal and trend components of the model, fitting only the intercept to the stable historic period.

To optimize the selection of the stable historic period, it was also needed to consider the method used for its selection. BFASTmonitor allows the user to choose among three methods. One of the proposed methods is the reversed-ordered-cumulative sum (CUSUM) of residuals (ROC) (Pesaran & Timmermann 2002). The ROC approach uses only the last observations of the historic period, and moves backward in time while calculating the cumulative prediction error of the model. It defines the start of the stable historic period at the moment in time when the model breaks down due to a structural change (Verbesselt et al. 2012). The advantage of this method is that it uses only part of the historic data, therefore allowing for a more accurate model to be fitted. However, it is not designed to detect with accuracy the time of a possible disturbance in the historic period, which means that it can be influenced by the presence of outliers. The stable historic period selected can be too short or not representative of the dynamics of the pixel (Verbesselt et al. 2012), therefore this approach was not used. Another alternative is to use the Bai and Perron method (Bai & Perron, 2003). The Bai and Perron approach can fit a linear regression with a certain amount of breaks to our time series. It allows estimating the unknown regression coefficients of the model together with the breakpoints. The advantage of this method is that it allows estimating with more precision the time of a possible disturbance in the historic period (Verbesselt et al. 2012). The Bai and Perron approach estimates the unknown coefficients of the model by minimizing the sum of squared residuals. The estimators of the breakpoints of the historic period are those that minimize globally the sum of the squared residuals over all the segments. In fact, an algorithm evaluates which partitions of the linear regression achieve a global minimization of the overall sum of squared residuals (Bai & Perron, 2003). However, it was not possible to implement this method to the data in R software.

Other alternatives are possible as well, that are similar to the Bai and Perron approach but are too computationally extensive (such as applying BFAST to the historic period to estimate with more accuracy the disturbances in the historic period) or are not automated (such as using expert knowledge of the area to manually select the historic period) (Verbesselt et al. 2012). Another aspect to consider of the area and data is the abundance of gaps and outliers. Even though curve fitting approaches like BFASTmonitor can help remove the remaining noise (Geerken, 2009), large data gaps may cause strong oscillations in the harmonic model (Brooks et al. 2012), such as the one BFASTmonitor fits to the historic period. The accuracy of fitting harmonics to such irregular data is very low. Given that it is assumed that the pixels

were not deforested in the historic period, structural changes were not expected to occur during that time that could lead to wrong estimations of the model parameters (i.e. inaccurate stable historic period selected). The choice was to use the full length of the historic period as stable period, because this approach was more robust against outliers and against missing data, and was simple and computationally possible. Therefore after those considerations, the choice was made to use all the historic period as stable period and to fit a model to it that included only the intercept.

4.4-Validation approach

For the validation, independent random samples were generated for each BFASTmonitor result: half of the samples belonging to the Deforested class and the other half belonging to the Non Deforested class. The Deforested class refers to the pixels where BFASTmonitor signalled a break with negative magnitude. Similarly, the Non Deforested class, refers to pixels where BFASTmonitor did not signal a negative break (i.e. either signalled a positive break or did not detect any change). A total of 400 validation samples were generated per test (200 among the pixels of the Deforested class and 200 among those of the Non Deforested class) to validate the results before and after the removal of remnant outliers. The result after including information of the spatial neighbourhood was validated with 172 pixels belonging to the Deforested class of BFASTmonitor and 200 belonging to the Non Deforested class. The tests regarding the selection of control pixels in the monitoring period were validated with a total of 300 samples each (150 samples of each BFASTmonitor class)

The validation also utilized Landsat Surface Reflectance products of the data, (bands 1, 2 and 3) to produce True Colour composites of each acquisition with the band combination Red= band 3, Green = band 2, and Blue = band 1. An example is shown in Fig.5. Each validation sample generated was overlayed to several RGB plots, generated for different moments in time, in order to assign the sample to a class (Deforested or Non Deforested) in an independent way. The corresponding confusion matrices were finally derived, and used to compare the different results of BFASTmonitor.

Fig. 5 An example of the validation procedure. A validation sample (in red) is plotted over a True Colour composite of the study area based on Landsat Surface Reflectance products (date: 2008-06-27). The composite is created with bands 3, 2 and 1 in R software.

4.5-Spatial context approach

In the main part of this study, it was assessed whether correcting the signal of pixels to remove the effect of external disturbances in the time series improved the detection of deforestation with BFASTmonitor in the area. The objective was to produce time series where the effect of external disturbances was minimised, and test whether the use of such time series could improve the detection of deforestation with respect to the previous results obtained after removing remnant outliers.

4.5.1-Pixel-based Regeneration Index (pRI)

We aimed to produce time series where the effect of external disturbances was minimised. The correction of time series can be done using the pixel based Regeneration Index (pRI) of Lhermitte et al (2010), which has the advantage of not depending on static reference data and of considering each pixel independently. This index also quantifies vegetation regrowth and heterogeneity within a deforested plot (Lhermitte et al. 2011). For this, the pRI employs information of reference pixels located close to the considered focal pixel. It is based on the assumption that the vegetation growth of the reference plots indicates the pattern of vegetation growth in the focal pixel, in case the focal pixel had not been deforested.

Reference pixels, called also control pixels, are therefore used as predictors of vegetation growth in the focal pixel. Therefore, the pRI index masks out possible external influences in the focal pixel (Lhermitte et al. 2011), and any change that may be present in the focal pixel can be interpreted as due to deforestation and to the following regeneration. The pRI is calculated with the following formula for the pRI:

$$pRI^t = {VI^t_{focal}}\Big/{VI^t_{control}} \qquad (1)$$

where VI^t_{focal} is the NDVI value of the focal pixel at the moment t and $VI^t_{control}$ is the mean vegetation index of the selected control pixels at moment t.

4.5.2-Similarity analysis approach

The Fig.6(A) below shows an overview of the conceptual approach for the similarity analysis approach. First the analysis focused on the historic period of a certain focal pixel and of the pixels within its neighbourhood. The purpose was to identify neighbours that presented a similar evolution of vegetation for that period of time as the focal pixel. The reason behind this is that those selected neighbours would predict the temporal pattern of vegetation in the focal pixel in the monitoring period with better accuracy than the other neighbours. They ensured that the pRI time series of the focal pixel would not present the effect of environmental disturbances in the monitoring period. The selected neighbours are referred to as x_H pixels (see Fig.6 (A)).

In the next step only the monitoring period of the focal pixel and of the x_H pixels (neighbours selected in the previous step) was considered. The x_H pixels selected may or may not be similar to the focal one in the monitoring period, resulting therefore in three different possible scenarios (depicted in Fig.7.). The first scenario (Case 1 of Fig.7) would occur when the focal pixel is deforested while most of the x_H pixels were not. This would produce pRI values close to 1 before the deforestation event. During the deforestation and recovery process, pRI values would decrease and increase, respectively. Once the recovery process has finished, values would again fluctuate around 1. Given that the pRI is calculated with the average of the x_H pixels, the behaviour of a particular x_H pixel has relatively less importance, depending on the x_H amount selected. The second case scenario (Case 2 in Fig.7) corresponds to the situation

where all the pixels involved (focal and x_H) belonged to a deforestation plot. They would remain similar throughout the monitoring period, and the pRI time series would be relatively stable around the value 1. The third possibility (Case 3 in Fig.7) involved the focal pixel not being deforested while most of the x_H pixels were.

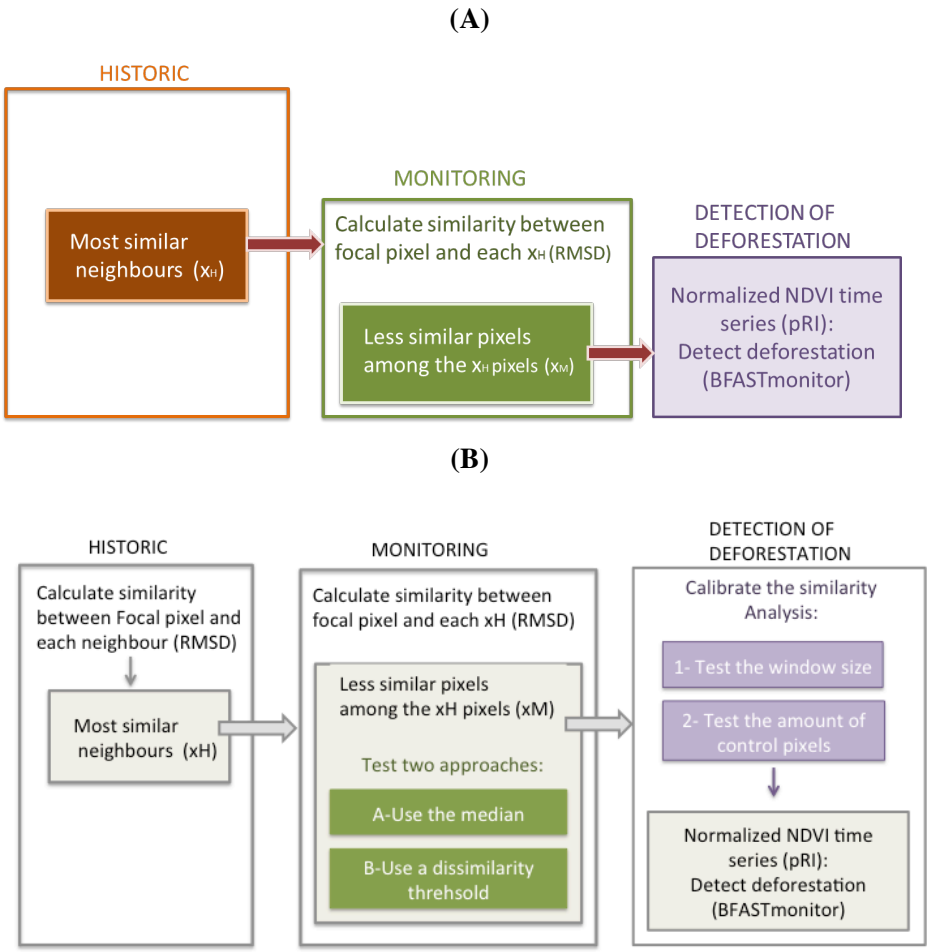

Fig. 6 Flowchart of the three steps involved in the spatial analysis. **(A)**:Overview of the process. First the effect of external disturbances in the historic period is removed by selecting, those neighbouring pixels with higher temporal similarity with the focal pixel (x_H pixels).Second, to ensure that neighbouring pixels affected by a change are discarded, only those x_H pixels with less similarity considering only the behaviour during monitoring are selected. Finally, the pRI time series is calculated. **(B)**: Flowchart of the steps taken in the spatial analysis, detailing the tests performed to optimize the selection of control pixels during the monitoring period. To select the least similar neighbours to the focal pixel during the monitoring, two approaches are tested (the Median Approach and the Dissimilarity Threshold Approach), that aim to discard the neighbours affected by a change (e.g. deforestation) during the period of monitoring. Next, a calibration of the pRI is performed, to adjust the window size and amount of control pixels used to the characteristics of the area.

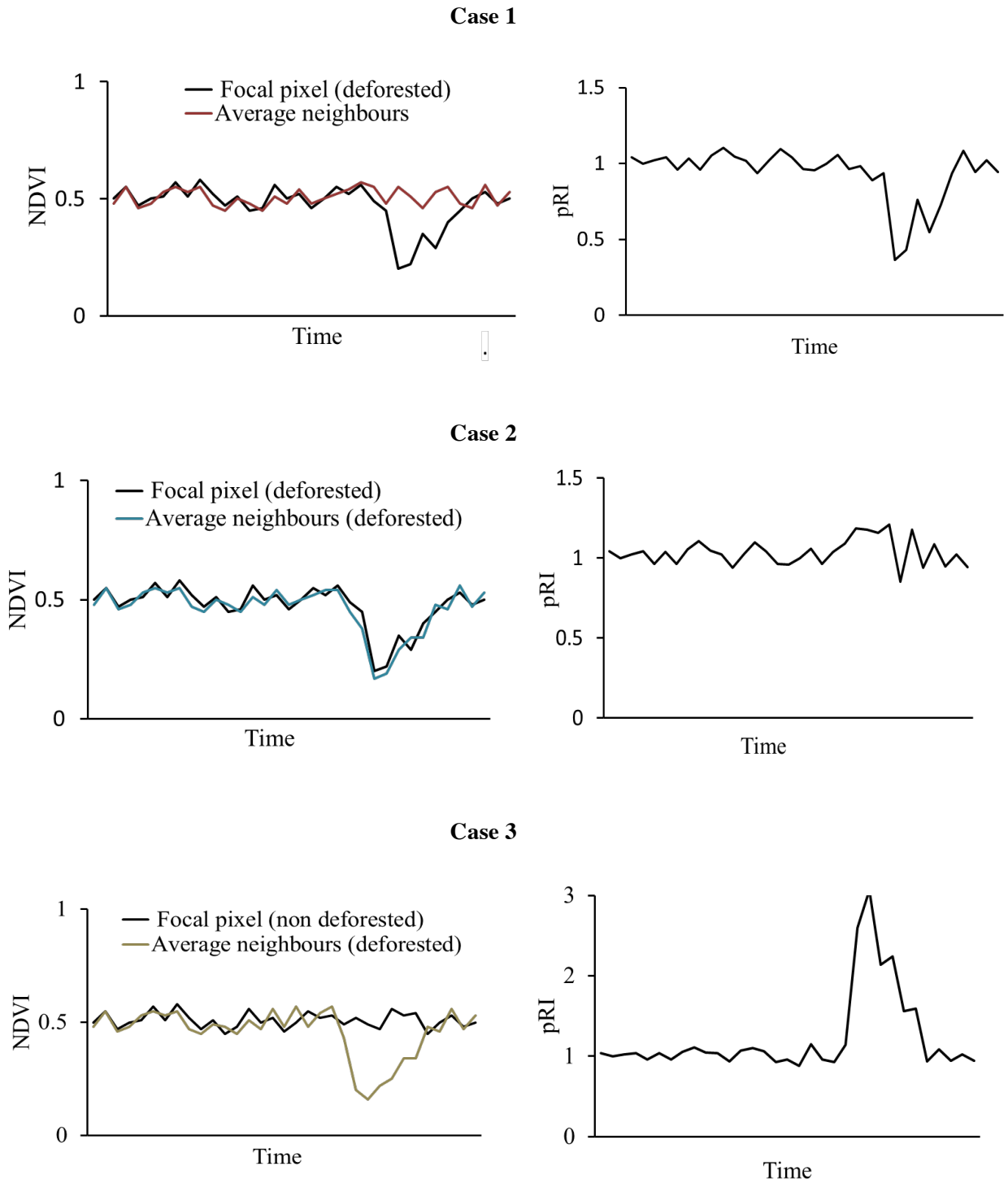

Fig. 7 Three possible case scenarios occurring during the selection of control pixels in the monitoring period. **Case 1:** the focal pixel is deforested while most of the control pixels selected based on the historic period (called xH pixels) were not. The pRI remains close to 1 in the historic period and drops during the deforestation event in the monitoring before the deforestation event. **Case 2:** all the pixels involved (focal and xH) belonged to a deforestation plot. The pRI remains relatively stable during the monitoring period, fluctuating around 1. **Case 3:** the focal pixel is not deforested during the monitoring period while most of the xH pixels are. The pRI shows a change of positive magnitude.

This would result in a pattern directly opposite to that of the first case scenario, because pRI values would then increase during deforestation and decreasing during recovery. Only the first scenario was of interest, because the pRI could then show a negative drop during the time of deforestation, which may be detected as structural change by BFASTmonitor. To ensure that the focal pixels analysed belonged to the first scenario, a selection was made among the x_H pixels (which were similar to the focal one only in the historic period) to obtain a certain x_M amount of pixels corresponding to those x_H pixels that were dissimilar to the focal one in the monitoring period ($x_H > x_M$). The selection of x_M pixels was delicate and involved certain criteria. A certain x_H pixel could be selected as x_M pixel if it was less similar to the focal pixel in the monitoring period than in the historic period. In addition to this, it was necessary to add an extra criterion to guarantee that the x_H pixel analysed was not deforested, and to therefore reduce noise in the pRI time series for the monitoring period. We tested two approaches: the Median approach (Approach A) and the Dissimilarity threshold approach (Approach B), and selected the approach that returned the most accurate results. Both approaches are detailed further below. The x_M pixels finally selected were the reference (or control) pixels, and were used to calculate the pRI time series over both historic and monitoring period. This pRI time series was the input for BFASTmonitor. Later on, we validated this BFASTmonitor result and compared it with previous runs.

4.5.2.1-Similarity measure

A correct selection of neighbouring pixels (x_H and x_M) is essential, and is performed by analysing the similarity between the time series of the focal pixel and that of the neighbouring pixel. For that, we relied on the Root Mean Square Distance (RMSD) as similarity measure. The RMSD calculates the distance between corresponding observations along the time series. In case one of the observations is missing, the RMSD does not take it into account. In this way RMSD accounts for missing values and provides a robust estimation of similarity between irregular time series. The RMSD takes into account the within-class heterogeneity caused by local ecological differences, as well as amplitude translations resulting from different backgrounds (soil type, understory vegetation) (Lhermitte et al. 2010).

After a preliminary analysis in a few random samples, the necessity to reduce the noise in the pRI time series during the historic period was evident. We needed to select as x_H pixels the

most similar neighbours of a focal pixel, and furthermore those neighbours needed to be as similar as possible. We therefore used a threshold in this selection, of RMSD = 0.0025. This criterion ensured that only neighbours with RMSD values lower than 0.0025 were selected for the next stage. This analysis was identical for the following tests and steps.

4.5.2.2-Selection of control pixels in the monitoring period

As stated above, in the monitoring period, it was important to optimize the selection of the x_M pixels to reduce the risk of false detections. Two different approaches were developed and tested: the Median Approach and the Dissimilarity Threshold Approach. In the first stage of the spatial analysis this was done with a fixed window size and fixed amount of control pixels x_M. Fig. 6(B) details the tests we performed in the monitoring period and the tests related to the calibration of the similarity analysis. The calibration tests are explained further below. The objective of the Median and the Dissimilarity Threshold Approaches was to produce pRI time series with reduced noise in the monitoring period, where the negative drop in the NDVI due to deforestation would be visible.

For that, it was necessary to ensure on one hand that the pixels selected for the calculation of the pRI were less similar to the focal pixel in the monitoring than in the historic period. On the other hand, it was important that pixels were not too dissimilar. In fact, if that was the case, the pRI time series in the monitoring period would not produce accurate detections. Both approaches were evaluated in a test site contained within the study area and validated independently. The most accurate one was chosen for the second stage of the spatial analysis. Approach B was applied in an additional test area, because the results of the first area did not contain enough pixels for the validation. In fact only 60 pixels had been signalled as deforested by BFASTmonitor in the test area, so it was applied it in a second test area and both validation results were combined to reach a total around 200 samples for each class. Approach B is very restrictive, when compared to Approach A, and only few pixels can be analysed with it.

A-Median approach

This approach uses the median NDVI over the monitoring period to select the x_M pixels that are more likely to not have suffered from deforestation during that time. The procedure is as

follows. For a certain pixel time series, the first step calculates the median NDVI over the historic period. This represents the undisturbed NDVI value of the pixel. Next, the procedure calculates the median NDVI over the monitoring period. After that, both median values are compared. It is assumed that non-deforested pixels present a higher median than those pixels that have been deforested. Based on this assumption, the approach aims to select those x_M pixels where the median NDVI value over historic and monitoring periods are as close as possible. In particular, the criterion used required a median NDVI value calculated over the monitoring period to be at least 80% of the value over the historic period.

B-Dissimilarity threshold approach

The Dissimilarity threshold approach relied on the use of two thresholds to define which degree of dissimilarity was the maximum accepted in the monitoring period. After a preliminary analysis in several random deforested samples, the value we used was of RMSD = 0.003. This allowed us to select control pixels that would produce a pattern of deforestation as recognizable as possible.

4.5.2.3-Calibration of Similarity Analysis: window size and amount of control pixels.

The neighbouring pixels for each part of the analysis (x_H and x_M) are selected based on time series similarity and spatial context. They are selected only within a certain neighbourhood of the focal pixel, referred to further on as window w_{k*k}, where k is the length of the window side. This is due to the underlying assumption that there is a decrease in the spatial correlation of environmental conditions when control pixels are selected further away from the focal one. This phenomenon is called window size effect (Lhermitte et al. 2010). Due to the window size effect, the window used needs to be small enough to ensure high spatial correlation between the neighbours and the focal pixel. At the same time, the window size had to remain big enough to guarantee that part of the pixels that fell within the window were not affected by deforestation. It was therefore necessary to define the window size. Furthermore, also the number of neighbouring pixels to use for the pRI calculation had to be defined, to ensure that we select only the most similar candidates by using the discrimination power of the VIt time series (Lhermitte et al. 2010). For that, three window sizes were defined and tested with a fixed amount of control pixels. Each result was validated and finally the most appropriate window size among them was chosen. Similarly, two different

amounts of control pixels were then tested and validated using the selected window size, and the one returning the most accurate results was chosen. After the calibration it was possible to determine which window size and which amount of control pixels among the values tested were the most appropriate for the characteristics of the data.. The accuracies of each test were judged considering the overall accuracy as well as the omission and commission errors. It is important to acknowledge that the values of the window size and of the amount of control pixels are an orientation. A sensitivity analysis should be run in order to define the optimal combination of both parameters for our study area. Furthermore, the results of our tests are difficult to extrapolate to other areas or studies.

4.6 Characterizing drought in the study area

In order to have a general understanding of the dynamics of climatic disturbances that may have affected the results, TRMM rainfall data were collected and used to estimate the occurrence of drought. Drought is in fact the main natural factor affecting ecosystems productivity in the context of climate change (Malhi et al. 2009) and the calculation was done using the standard precipitation index (SPI). This index presents the incremental rainfall deficit that originates drought at different timescales (McKee, et al. 1993). For the amazon forest, an SPI calculated at 6-months timescales is considered appropriate to distinguish incremental dry anomalies between the dry and wet seasons (Li et al. 2008).

5- Results

5-1-Removing remnant outliers: Preliminary tests on the temporal threshold

A literature review of the length of recovery processes after deforestation (Section 4.1) showed that the value of the temporal threshold should be shorter than one year. Therefore the effect on the detection accuracy of different temporal thresholds was analysed, using the following values for the threshold: 104, 272 and 303 days. The time of the detected change with BFASTmonitor for each case is presented in Fig.8. The detection of deforested areas achieved different overall accuracies with each tested value. A threshold of 104 days produced the most accurate result, with an overall accuracy of 87.25%, as well as the lower values for the commission error (equal to 7%) and for the omission error (equal to 5.75%). Opposite to this, the results of the highest value of the temporal threshold (303 days) produced the less accurate results: an overall accuracy of only 64.75% and higher commission and omission errors (respectively equal to 17.50% and 17.75%). The intermediate value of the temporal threshold (272 days) produced results that are in between those obtained with the shortest and the highest values, but that are nevertheless closer to the detection results of the highest temporal threshold tested (i.e. to 303 days). The overall accuracy reached using the 272 days threshold only reached 68.5%, and the commission and omission errors remained high, with values of13.50% and 18% respectively. After this test, the 104 days were chosen as the appropriate temporal threshold, and was applied in all next analysis.

5-2- Effect of removing remnant outliers: comparison before and after its application

First BFASTmonitor was applied to the data prior to the removal of remnant outliers, and the resulting map is shown in Fig.9(A). The detection of deforested areas achieved an overall accuracy of 87% and presented a relatively low omission error (4.5%) and commission error, which was slightly higher and reached 8.5%. After removing remnant outliers with the chosen temporal threshold of 104 days (see Fig.8 (A) for the detection map), the detection result showed a slight improvement in the overall accuracy, which increased to 87.25%. The commission error decreased to 7%. However, the omission error increased but remained relatively low (5.75%). The comparison of both cases, which is depicted in Fig.9 (B), and

illustrates the slight improvement obtained in the case where remnant outliers were removed. Therefore the approach to remove remnant outliers with a temporal threshold of 104 days was selected and applied in the following steps.

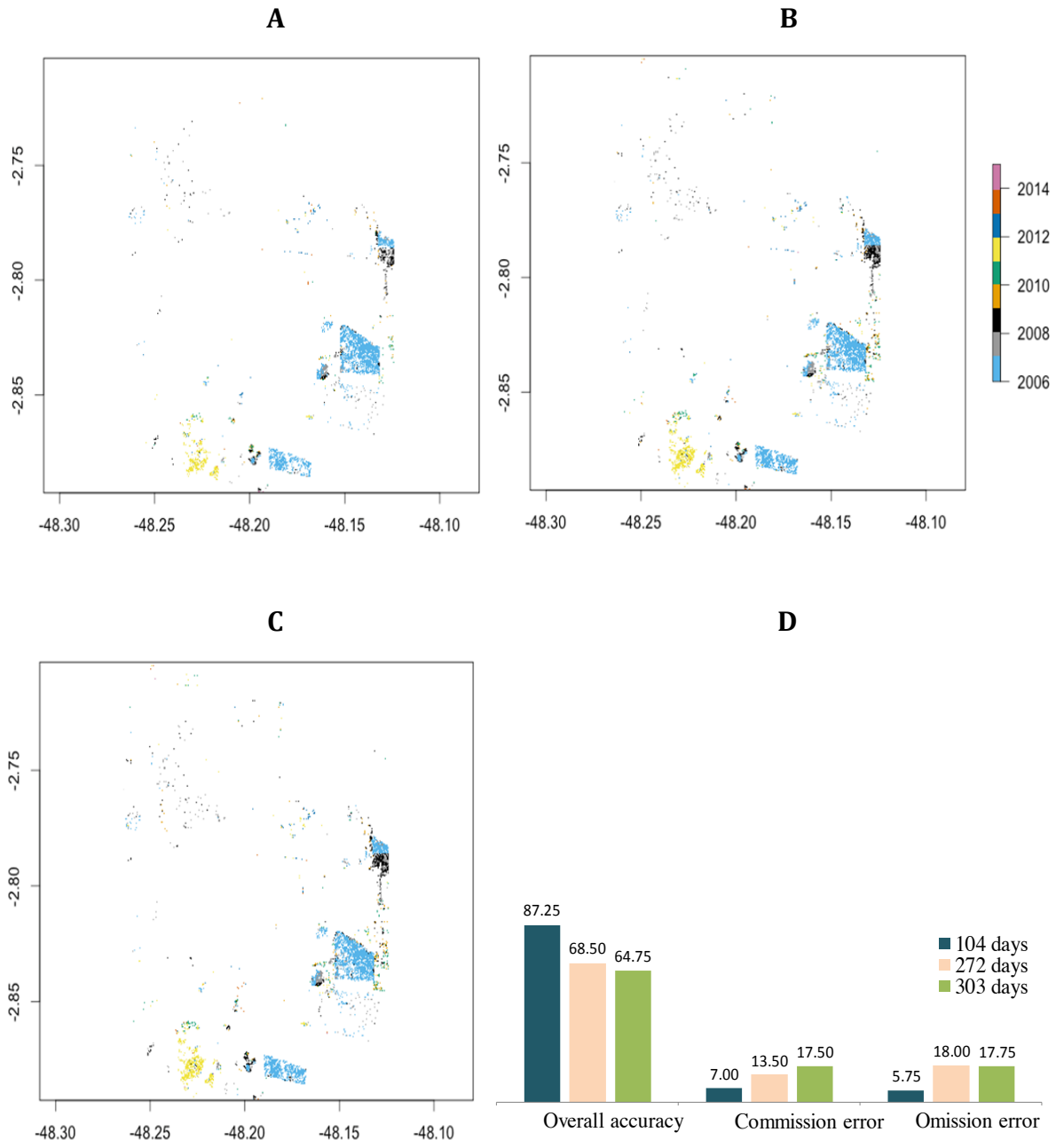

Fig. 8 Deforested areas detected by applying BFASTmonitor on NDVI time series where remnant outliers have been removed using different values of the temporal threshold: (A) 104 days, (B) 272 days and (C) 304 days). The graph shown in (D) compares the validation results of the three tests.

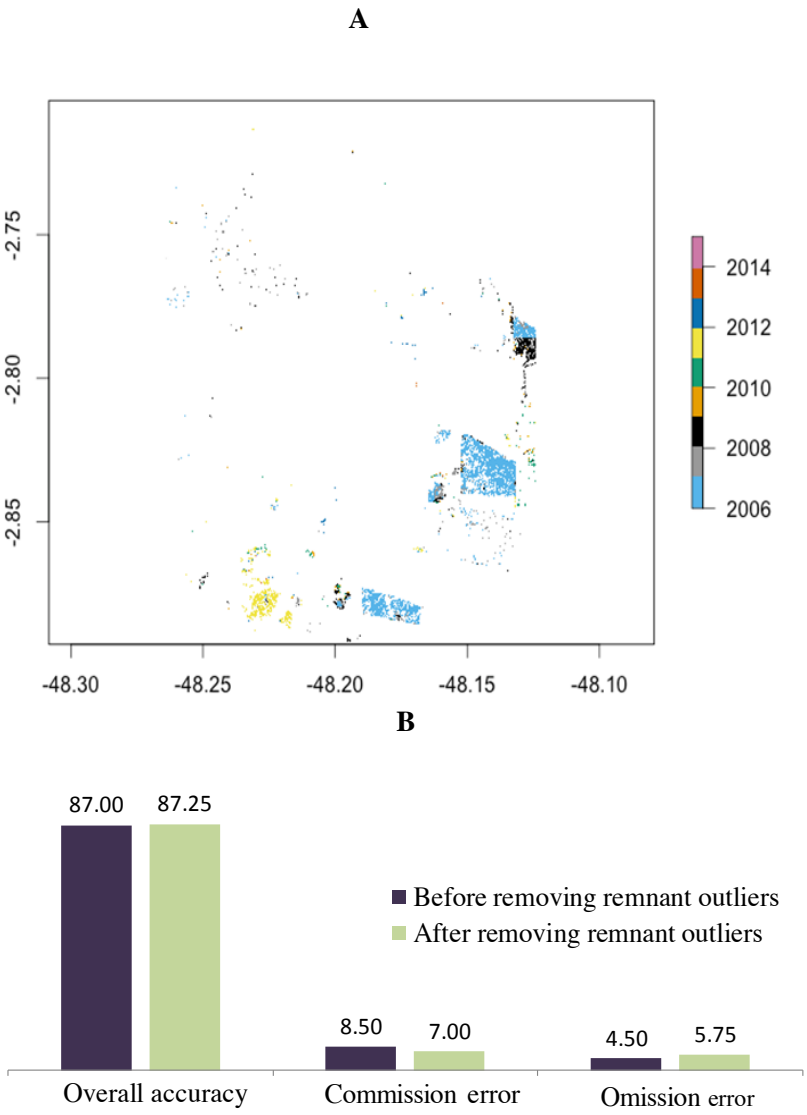

Fig. 9 Deforested areas detected by applying BFASTmonitor on NDVI time series where remnant outliers are present (A). The detection result obtained after removing the remnant outliers from the NDVI time series with the chosen value of the temporal threshold (104 days) is displayed in Fig.8(A). The graph shown in (B) compares the validation results both cases.

5-3- Selection of control pixels during the monitoring period: testing the Median Approach and the Dissimilarity Threshold Approach

The Median and Dissimilarity Threshold approaches were tested and validated to assess if they optimize the selection of control pixels in the monitoring period. Fig.10 shows the detection result with BFASTmonitor and the comparison of the validation results for the Median approach and for the Dissimilarity Threshold approach. The detection of deforested

areas with the Median Approach was significantly better than with the Dissimilarity Threshold Approach. The Median Approach reached an overall accuracy of 70.67% and a relatively lower commission error of 11.33%, respectively compared to 53% and 25.33% with the Dissimilarity Threshold Approach. The values of the user's accuracy were relatively similar, with an omission error of 18% for the Median Approach, as opposed to 21.67% obtained with the Dissimilarity Threshold Approach. Therefore the Median approach produced more accurate results than the Dissimilarity Threshold approach. However, the addition of this method decreased the quality of the detection compared to results after the removal of remnant outliers (shown in Fig 8 (A) and 9(B)). This may be due to the excessive presence of gaps in the time series of certain pixels, which can be appreciated in the example time series shown in Fig. 11. This example shows that the effects of including the Median approach vary depending on the pixel. The Example pixel 1 of Fig.11 (A) shows that the Median Approach can produce more stable pRI time series. Also, the detection is improved because the change detected by BFASTmonitor is negative, and corresponds to the change caused by deforestation, observed in the validation step. In this case, the Median Approach represents an improvement, compared to Fig.11 (B) where such approach is not used, and where the magnitude of the change detected is positive. However, the Example pixel 2 of Fig.11 (C) shows a situation where the Median Approach does not affect the detection (Fig.11 (D)). Between the two tests analysed, the Median approach was chosen as the most appropriate to optimize the selection of control pixels in the monitoring period.

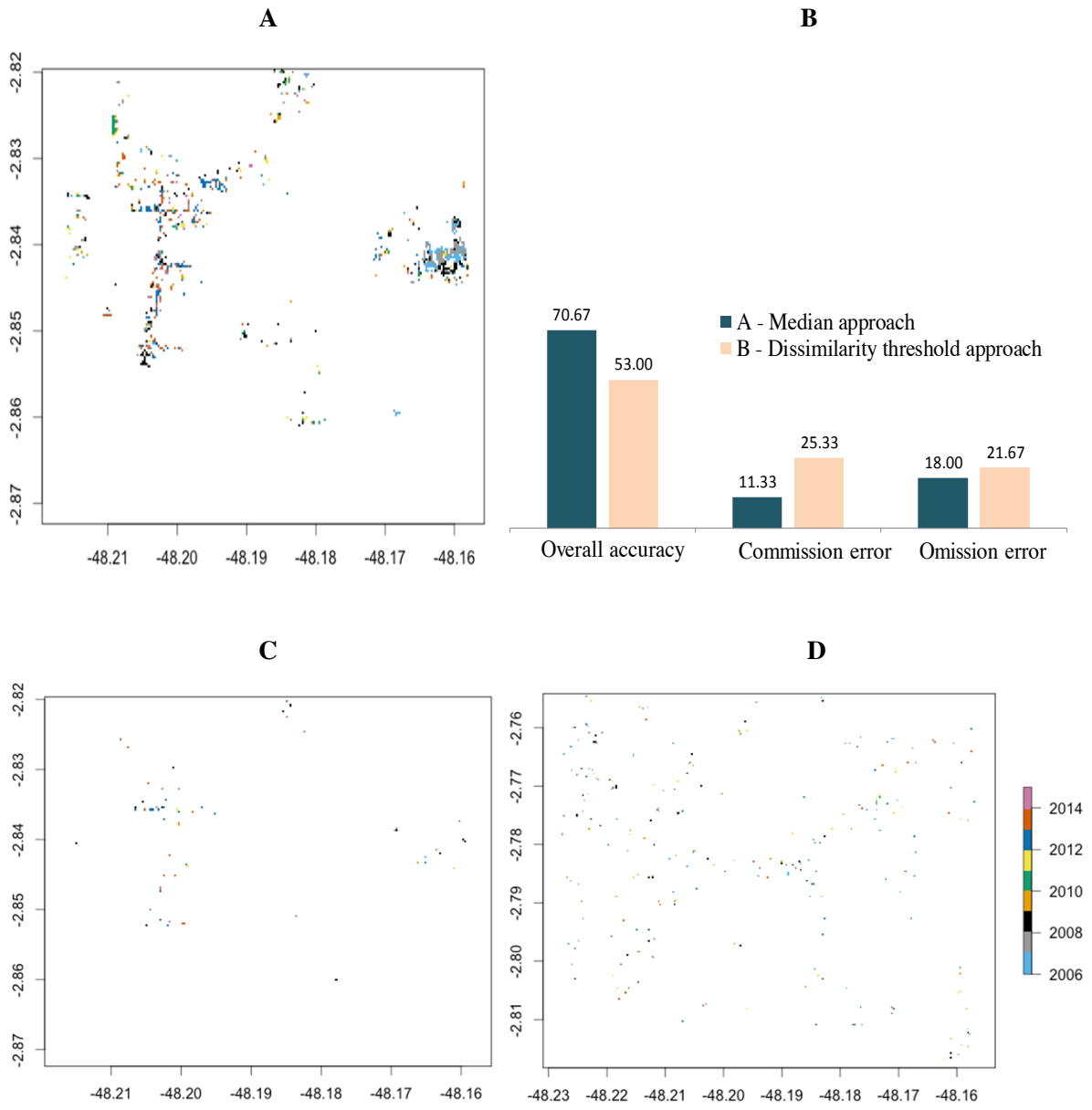

Fig. 10 Deforested areas detected applying BFASTmonitor on pRI time series which were calculated using different approaches to optimize the selection of control pixels in the monitoring period (see Section 4.5.2.2.) in subsets of the study area. For the calculation of the pRI the window size analysed was fixed in 7x7 and the amount of control pixels used was fixed in 6 pixels. (A): using the Median Approach in a subset of the study area, and (C and D) using the Dissimilarity Threshold Approach in two different subsets of the study area. In particular, (C) corresponds to the same subset of the study area as used in (A), and (D) corresponds to an additional subset, that was necessary to reach a minimum amount of processed pixels. The comparison of the three outputs is presented in (B).

Example pixel 1: deforested in year 2008

(A): without Median Approach: **(B): with Median Approach:**

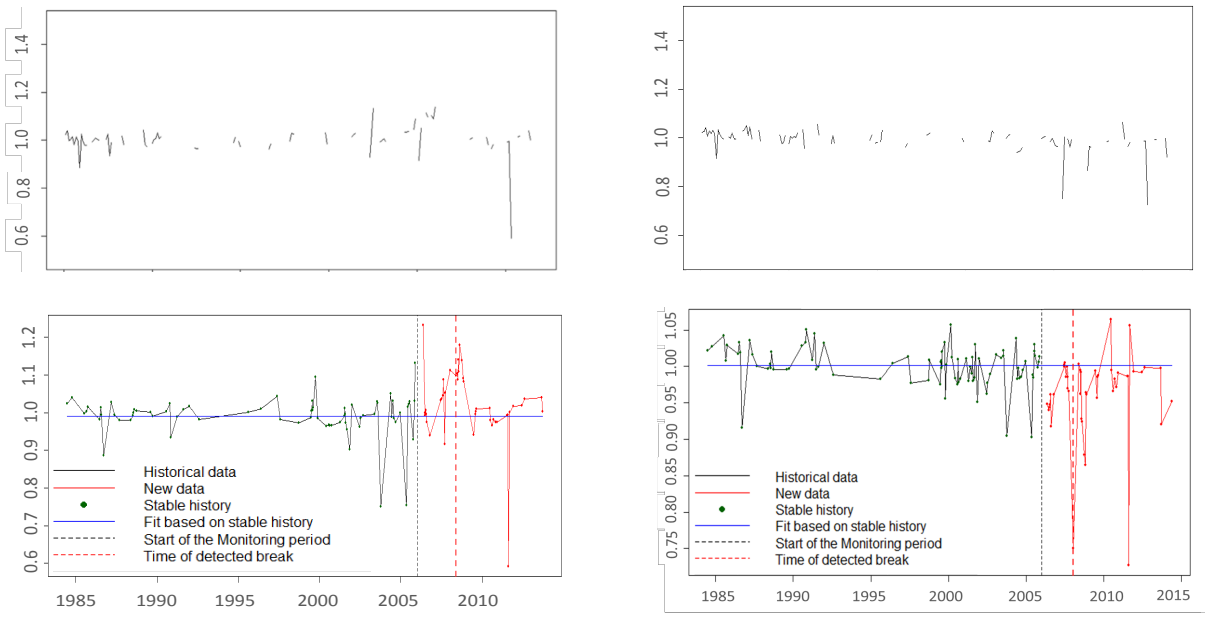

Example pixel 2: deforested in year 2007

(C) : Without Median Approach: **(D): With Median Approach:**

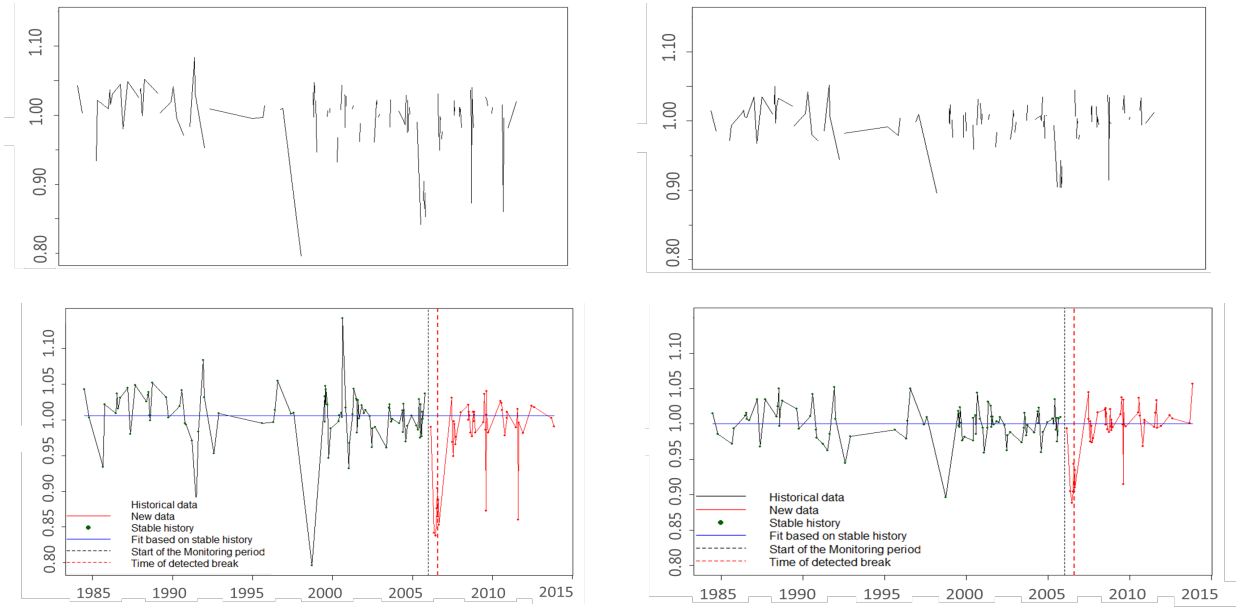

Fig. 11 Example of pRI time series and detection result with BFASTmonitor obtained on two pixels using 7x7 window and 6 control pixels. **Example pixel 1** was deforested during 2008. (A) shows that including the Median Approach improves the detection (with a pRI time series more stable, and negative change detected). In contrast, (B) shows the result when no Median Approach is used (noisier pRI time series and positive change detected). **Example pixel 2**, deforested in 2007, shows in (C) a case where the Median Approach does not affect the detection compared to the situation where no Median Approach is used (D).

5-4- Calibration of the pRI: window size and amount of control pixels

Next, we tested different window sizes in the test area, with the Median approach selected before. The window sizes chosen were of 7x7, 17x17 and 25x25. The corresponding detection maps for each test in the subset area are presented in Fig. 10(A), and 1.

The detection of deforested areas achieved different overall accuracies with each tested window. The smaller window (7x7) produced the most accurate detection results, with the higher overall accuracy (of 70.67%) and lower commission error (11.33%). The detection results obtained with bigger window sizes show less accuracy when the window size increases, while remaining in general terms similar to those produced with the smaller window size. The overall accuracy of the intermediate and biggest windows are indeed very close (respectively, 67.33% and 66.67%), as well as the commission errors (13.33% and 17.67% respectively). The omission error is optimal when the window size is the biggest (15.67), followed by the smaller window size (18%) and by the intermediate window size (19.33%). Hence the smallest window size tested, of 7x7, was chosen for the following steps. The comparison of the performance of the detection using a median approach for varying window sizes is summarized Fig. 12(B).

Finally the effect on the accuracy of varying the number of reference pixels selected for the calculation of the pRI was analysed. This was performed by testing two different amounts of reference pixels, equal to 6 and to 12 control pixels, while maintaining the window size fixed in 17x17. The corresponding detection maps in the subset areas are displayed in Fig.12(B) and 13(A).

The detection showed relatively similar results in both cases, but it was optimized when the amount of control pixels was smaller (6 pixels used) than when higher amounts were used (12 pixels). The overall accuracy reached was of 67.33%, in contrast to only 64% when 12 control pixels were employed. The commission and omission errors are also better in the case that uses 6 pixels. The results show indeed lower commission and omission errors in that case, which are 13.33% and 19.33%, as opposed to 14.33% and 21.67% when 12 control pixels are used. Therefore the amount of control pixels used for the pRI calculation was 6. The comparison of both tests is shown in Fig. 13(B).

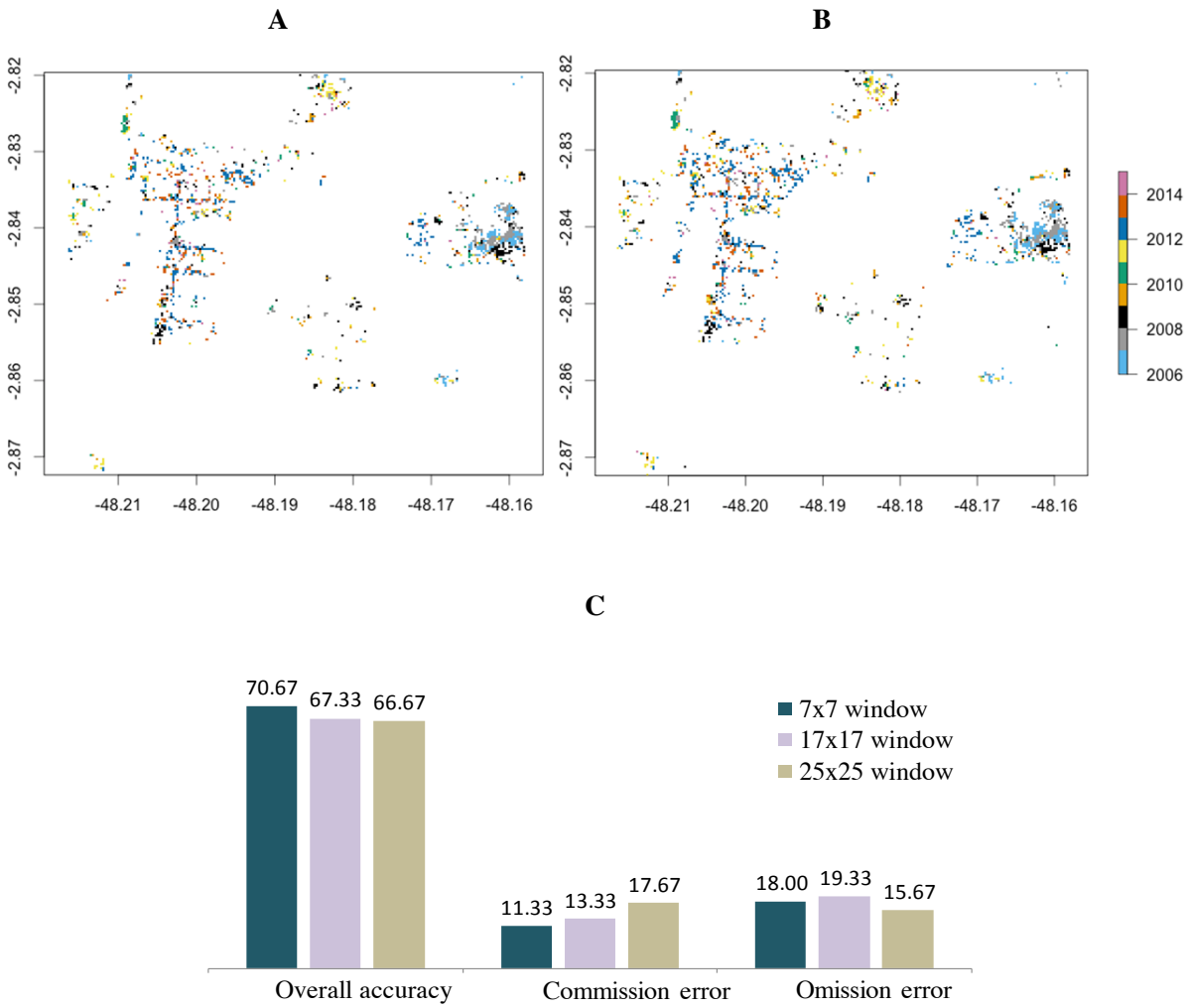

Fig. 12 Deforested areas detected applying BFASTmonitor on pRI time series which were calculated using different window sizes. The pRI time series were obtained using the Median Approach, which is used for the selection of the control pixels in the monitoring period (Section 4.5.2.2). For the pRI calculation, in this case, the amount of control pixels used was fixed in 6 pixels, and the window size analysed varied: (A) 17x17 and (B) 25x25. The detection map resulting from a test with window size of 7x7 are shown in Fig 10(A). The graph shown in (C) compares the validation results of the three outputs.

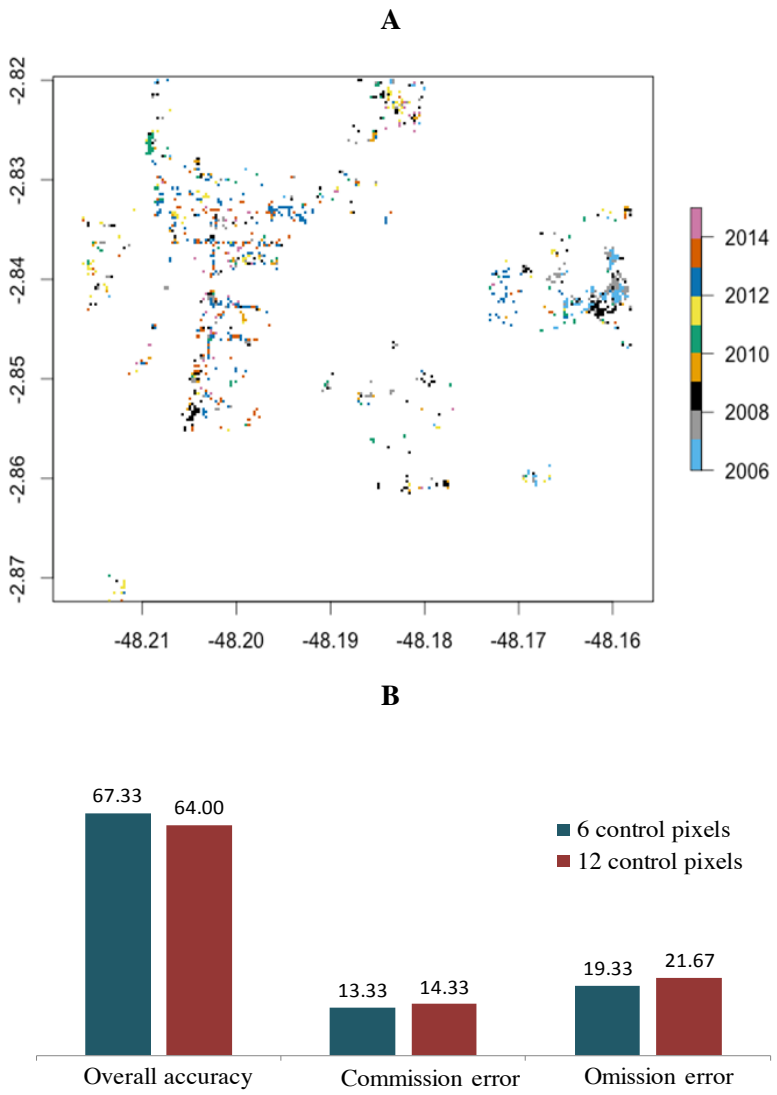

Fig. 13 Deforested areas detected applying BFASTmonitor on pRI time series which were calculated varying the amount of control pixels. The pRI time series were obtained using the Median Approach, which is used for the selection of the control pixels in the monitoring period (Section 4.5.2.2). For the pRI calculation, in this case, the window size was fixed in 17x17 and the amount of control pixels varied: (A) using 12 control pixels. The detection map resulting from using 6 control pixels is displayed in Fig.12(A). The graph shown in (B) compares the validation results both cases.

5-5- Effect of including information of the spatial context

In the second stage of the spatial analysis the results of those previous tests were used to implement the approach in the study area. Deforestation was detected with BFAST monitor including a spatial analysis performed with the Median approach a 7x7 window size and 6 reference pixels for the pRI calculation. The detection map resulting is shown in Fig 14. The

overall results obtained after including the spatial context represent a strong decrease in the detection accuracy, compared to the approach where remnant outliers were removed from the NDVI time series but no spatial context analysis was implemented. The overall accuracy drops from 87.25% in the case of no spatial analysis to 59.68% when such analysis is included. The commission and omission errors are dramatically increased, with commission errors that increase from 7% to 17.74% respectively and omission errors rising from 5.75% to 22.58% respectively. Fig.14 (B) compares the detection results of both cases, allowing seeing the effect of including the spatial context analysis in the detection. Fig.15 presents the time series of a pixel where the detection was correct after removing remnant outliers, but where including the spatial analysis produced a wrong detection. The historic period of this pixel presents a drop in the NDVI value around year 1990, which may be due to a deforestation event that was not detected with the VCF and FCC layers.

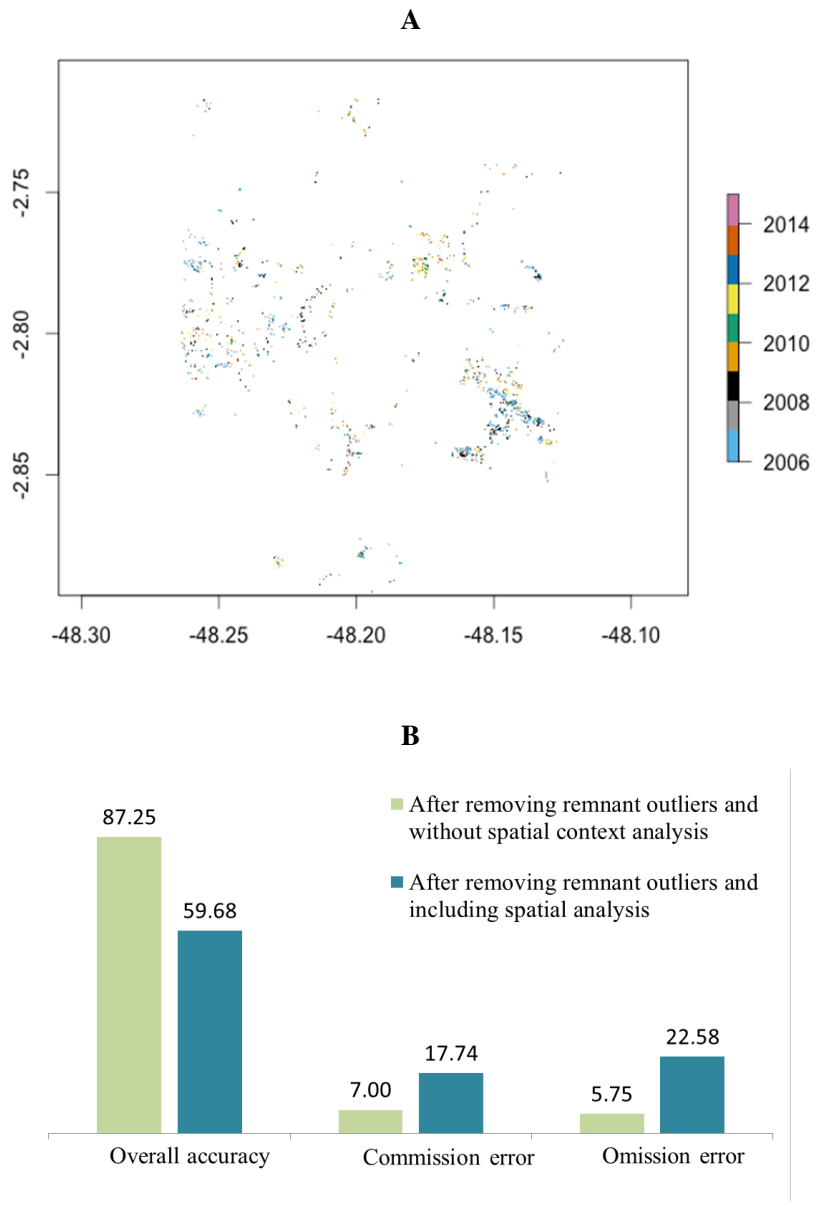

Fig. 14 Deforested areas detected with BFASTmonitor after an analysis of the spatial neighbourhood of each pixel was carried to produce pRI time series. The pRI time series were calculated as follows: First remnant outliers were removed from NDVI time series with a temporal threshold of 104 days. Next, pRI time series were derived using a 7x7 window size and 6 control pixels. The calculation of the pRI included an implementation of the Median approach for the selection of control pixels during the monitoring period (Section 4.5.2.2). The comparative deforested areas were detected applying BFASTmonitor on NDVI time series where remnant outliers had been removed using the optimal temporal threshold (104 days) is shown in Fig. 8 (A). The graph shown in (B) compares the validation results both cases.

1- Detection after removing remnant outliers

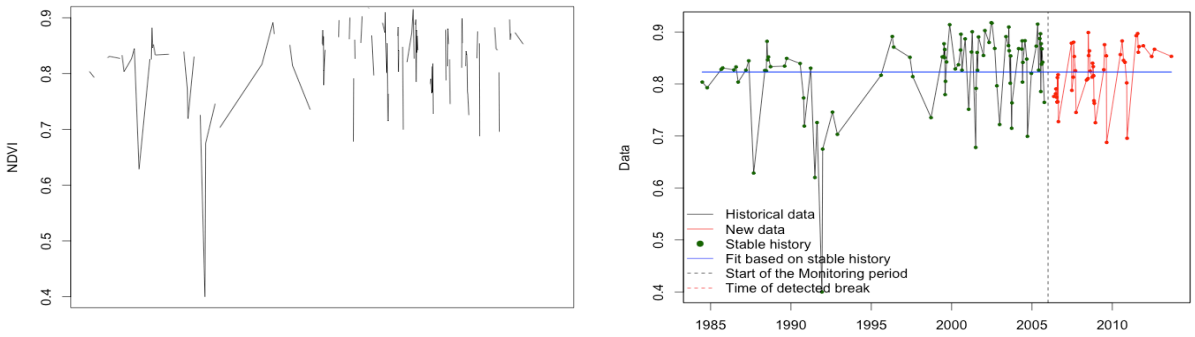

2- Detection after removing remnant outliers and including a spatial context analysis

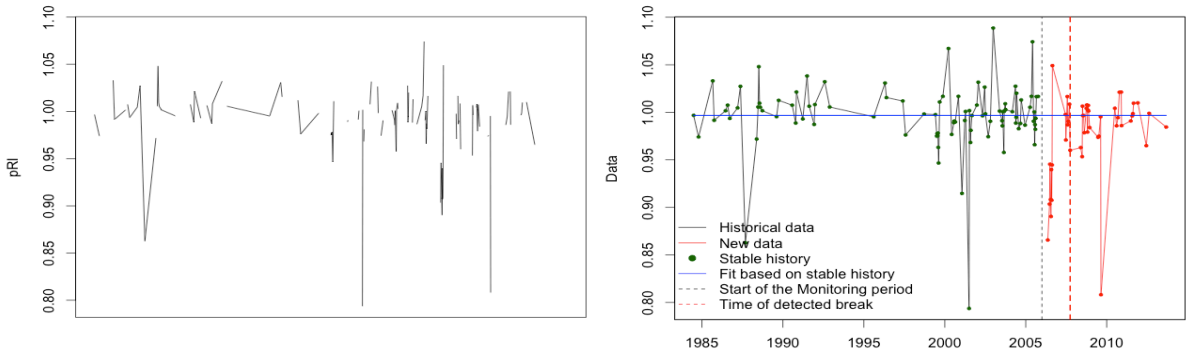

3- Validation

Fig. 15 Example pixel illustrating the effect of the spatial analysis on the detection with BFASTmonitor.(1) Shows the NDVI time series and detection result after removing remnant outliers, where no change is detected. (2) Presents the pRI time series and detection result after the spatial context analysis, where a change is detected in the end of year 2007. However the validation procedure does not reveal a change, as shown in (3), where the validation sample is overlaid with an RGB composite of a Landsat image at the beginning of year 2008. The change detected in (2) is therefore wrong.

5-6- Occurrence of drought in the area

The occurrence of drought in the area was estimated by calculating the SPI with a time step of 6 months, based on monthly rainfall data (TRMM). The resulting time series is shown in Fig.16, and illustrates the occurrence of moderately dry and extremely dry drought events around years 2009 and 2010 respectively.

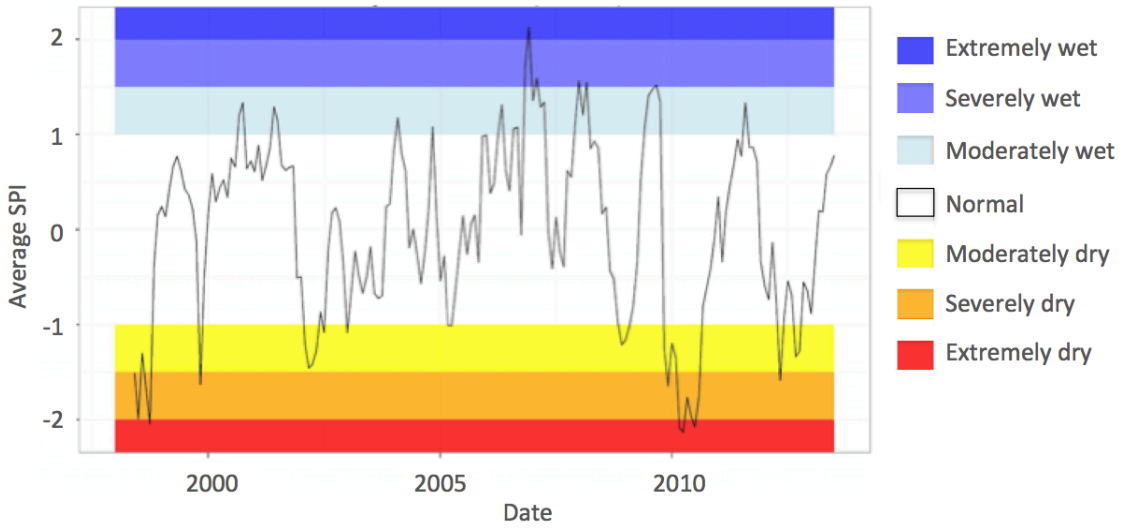

Fig. 16 Detection of drought occurring in the area with SPI time series. The calculation is based on Level 3 TRMM data from1998 to 2013, recorded monthly. The TRMM data are available freely from the NASA-Goddard Earth Sciences Data and information services Centre (http://disc.sci.gsfc.nasa.gov).

6- Discussion

This study does not draw clear conclusions of whether the temporal threshold approach can remove remnant outliers in a way that improves the detection of deforested areas with BFASTmonitor. On one hand, the detection results of applying such temporal threshold are slightly more accurate than the detection results where no temporal threshold has been applied (section 5.2). On the other hand, the improvement is very subtle and therefore may be due to the normal variation of the validation data collected.

Shorter temporal thresholds remove a smaller amount of observations and produce also more accurate detection results in comparison to larger thresholds. Hence it is important that the temporal threshold approach remains conservative towards the data, to avoid removing data that do not correspond to noise or that can be used accurately by the detection method despite corresponding to an outlier. Besides, it is reasonable to expect that values shorter than the one used in this study could produce better results, up to a certain limit. The lowest accuracy was achieved when spatial context is used, compared to the cases where no spatial context analysis was performed. The main reason behind this lack of improvement is attributed to the noise present in the pRI time series during the monitoring period. This is explained by the presence of excessive noise in the Landsat NDVI time series, due to undetected clouds and other external disturbances occurring in the time of monitoring.

Clouds are acknowledged to be a problem for forest monitoring in the tropics (Gu et al. 2012; Gu et al. 2009; Kennedy et al. 2010; Michishita et al. 2014; Poulter & Cramer 2009). Previous research applied BFASTmonitor on Landsat data of tropical areas of Ethiopia and could produce accurate results without relying on gap-filling methods (DeVries et al., 2013). However, cloudiness in Landsat data can as well cause the detection of abnormal changes, and cloud masking remains a critical challenge when monitoring deforestation with BFASTmonitor in the tropics (Reiche et al. 2015; Romijn et al. 2012). Current clouds screening methods for Landsat data are not comprehensive (Hagolle et al. 2010; Zhu & Woodcock, 2012) and the results depend on the data type and site (Schultz et al. 2013). The method proposed here is simple and consists on a conservative threshold-based approach for Landsat data that discriminates clouds from real changes. It is tested by assigning different values to the temporal threshold, all shorter than a year. The choice of values shorter than a year is supported by other studies in literature. For example the work of Kennedy et al.

(2010) assumes that artificial changes do not last more than a year. Similarly, Huang et al. (2010) consider the time for the reestablishment of a new forest stand as superior to a year (at least a couple of years). Also Poulter & Cramer (2009) considered very short temporal thresholds by defining a certain variation in the index as unrealistic if it occurs within a period of 6 weeks. Furthermore, the results illustrate that the more conservative temporal threshold values (i.e. the shorter values) produce more accurate results. This coincides with previous findings of Reiche et al. (2015) who showed that the accuracy of detecting deforestation with Landsat with BFAST monitor decreases when the amount of missing data increases. The study applies BFASTmonitor on Landsat irregular data over the tropics. In accordance with previous studies (DeVries et al., 2013), the detection of deforestation in a tropical area before removing remnant clouds was effective despite the presence of outliers, with an overall accuracy of 87 %. The temporal threshold method to remove remnant outliers produced a slightly more accurate detection of deforestation than in the case where no removal of remnant clouds was applied. However, this is not necessarily due to the effect of the temporal threshold. It may be due to the validation procedure, where independent sets of validation samples were created, and therefore may reflect the normal variation between samples. However, results also showed that most of the noise is not removed or smoothed from the NDVI time series. This was in line with our expectations, because of the simplicity of the remnant cloud removal approach and because previous authors had already highlighted the importance of data preprocessing to produce reliable and high quality NDVI time series from Landsat and improve deforestation detection with BFASTmonitor (Schultz et al. 2013; Verbesselt et al. 2012). Furthermore, this result is similar to the findings of previous studies. Kennedy et al. (2010) presented an algorithm to separate ephemeral change from real change. They acknowledge the fact that Landsat time series still presented important persistent cloudiness or gaps after applying their cloud screening algorithm. In such cases, they adapted their approach to detect changes in longer time scales.

BFAST monitor can detect deforestation in the tropics (DeVries et al., 2013) but has the potential to be further improved by a correction of the effect of external disturbances based on a spatial context analysis (Lhermitte et al. 2010). Here, we proposed to combine BFASTmonitor, which is a monitoring approach robust against missing data, with a pixel based regeneration approach that can remove the effect of external influences in the time series. The external disturbances can be caused by uncertainties in the radiometric or

atmospheric corrections as well as by topographic effects, vegetation phenology or climatic events (Lhermitte et al. 2011). The pRI has previously been used for fire assessment purposes with different sensors and indices (Lhermitte et al. 2011; Veraverbeke et al. 2010, 2011, 2012). However it has not been tested for NDVI data from Landsat in tropical areas and it has not been combined with BFASTmonitor for the purpose of monitoring deforestation. Our results show that a small window size (7x7) and a small number of control pixels (6 control pixels) produce more accurate results with BFASTmonitor for the case studied here. It can be explained as follows. In bigger window sizes, pixels distant to the focal pixel can be selected as control ones but may have different meteorological conditions than the focal pixel during the monitoring period, and can therefore be dissimilar (Lhermitte et al. 2010; Veraverbeke et al. 2010). Also, regarding the amount of control pixels, this can be explained by a finite beneficial effect of averaging, that smoothens out random noise and produces a more stable pRI time series, which is also more similar to that of the focal pixel. However, using a too large number of control pixels will decrease the similarity because it will introduce pixels that are not so similar in the calculation (Veraverbeke et al. 2010). Previous studies found similar results concerning the calibration of the pRI for their particular cases (Lhermitte et al. 2011; Veraverbeke et al. 2010). However, they used different data and study area. Both Veraverbeke et al. (2010) and Lhermitte et al. (2011) relied on Landsat sensors but did not use the NDVI, did not monitor deforestation and did not do it in tropical areas. The same theoretical background supports the results of this study, but the numerical comparison between our study and that of Veraverbeke et al. (2010) and Lhermitte et al. (2011) is not applicable due to the difference in data and study area. In fact the calibration results depend on the spatial resolution of the data and on the scale of the vegetated areas (Lhermitte et al. 2010). The correct window size for the whole area depends on the location of the affected pixels in the affected area or patch (Li et al. 2008; Veraverbeke et al. 2010). Pixels close to the boundaries of the patch will require smaller window sizes. Similarly, pixels in the middle of large patches will need larger window sizes (Veraverbeke et al., 2010). The area analyzed here did not present big deforested areas during the monitoring period, because most of the large patches were deforested previously and were therefore masked out from the analysis (they did not belong to the class forest). This can explain the fact that the best window was the smallest one. Previous studies (Veraverbeke et al., 2010) mention that the accuracy may be better close to the perimeters of the affected areas, because the window size is smaller and the pixels contained in it are expected to be more similar than in bigger windows. Authors

signal that it is inevitable, since in the middle areas of the patch, the potentially most similar pixels have also been affected by the change. (Veraverbeke et al. 2010). Our results show that the pRI produces worse detections with BFASTmonitor when compared to the situation where no spatial context is included. In general, the pRI time series are relatively stable during the start of the historic period, but become highly noisy towards the end of the historic period as well as during the monitoring. Other studies have reported noise in the pRI time series derived from Landsat, and the implications of it differ per case. Some do not signal a need to reduce noise (Veraverbeke et al., 2010), probably due to the choice of a study area outside of the tropical region. On the other hand, other studies acknowledge the importance of removing external influences when using Landsat products, and recognize the pRI as able to provide valuable representations of regeneration processes when data different than Landsat are used, prioritizing the use of moderate to coarse spatial resolution are used (SPOT or MODIS) (Lhermitte et al. 2011). In this case, studies that develop approaches to remove noise from pRI time series are extremely rare, with only the work of Lhermitte et al. (2011), which assessed regrowth after fire events in savannah ecosystems with SPOT-VEGETATION NDVI data. The authors used an integrated change approach to assess intra-annual dynamics of the regrowth. Such approach uses integrated metrics of intra-annual dynamics, that the authors derived from the SPOT data using pRI time series, and can remove random noise from the pRI time series. The authors recognize that, even though this technique is robust to noise, it needs to be tested and refined for different ecosystems. In fact, the environmental and change event characteristics will vary for different areas. Therefore the interpretation of the presented technique is likely to vary as well (Lhermitte et al. 2011). Following this recommendations, further research could investigate whether the approach proposed by Lhermitte et al. (2011) can significantly reduce noise in pRI time series calculated from Landsat data of tropical areas, where cloudy and missing observations are numerous, and assess the performance of BFASTmonitor on them.

There is no evidence in literature of other approaches similar to the Median approach being employed to distinguish deforested from non-deforested pixels in pRI. Despite this, the use of the median is regarded as more robust against variations in the data than other measures by other studies (Lhermitte et al. 2010). Also, previous studies carried relatively similar approaches to find areas where the percent tree cover was changed, that used the mean and standard deviation instead of the median (DeFries et al. 2002). In the mentioned study,

several training sites were used to calculate the mean percent of tree cover. Next, two particular values of the percent tree cover were compared. In case their difference exceeded two standard deviations from the mean, a change was signaled.

As signaled previously, the noise that is particularly present in some parts of the pRI time series (particularly during the monitoring period and the end of the historic period) can be due to external disturbances that started and evolved during that time. The SPI is designed to represent drought at any time scale (McKee et al. 1993) and has been used to detect droughts in the amazon (Zeng et al., 2008). The SPI results (Fig.15) show the occurrence of a severe drought around year 2010 in the area. There is evidence in literature that a previous very severe drought occurred in 2005 in the southern two-thirds of Amazonia, which was driven by an elevated sea surface temperature in the tropical Atlantic ocean (Marengo et al. 2008; Phillips et al. 2009). The fact that this drought did not affect directly the northern regions of Brazil (Marengo et al. 2008), where our study area is located, explains why the SPI does not reflect the episode. The drought detected in 2010 by the SPI is in accordance with previous findings (Marengo et al. 2011), which describe a widespread drought taking place in the Amazon in that year, due to an El Niño event that was intensified because of warming of the North Atlantic ocean (Marengo et al. 2011). Despite the SPI results, the link between the droughts detected and the noise present in the pRI time series during the monitoring period is not clear. Scientists recognize changes in the intensity and length of dry seasons in the Amazon, and connect such changes with lower river water and discharge levels (Marengo et al. 2011). They acknowledge in a general way the possibility that they cause profound environmental impacts (Marengo et al. 2011), namely through increases in tree mortality (Nepstad et al. 2007). However, it is difficult to deduce that droughts are having such an environmental impact from our pRI data. On one hand, the drought of 2010 was reported to have caused lower precipitation levels, lower streamflow levels, higher surface temperatures and increased evapotranspiration (Marengo et al. 2011), but the pRI time series do not show a clear pattern reflecting such changes in the pRI time series around year 2010. Also, Marengo et al. (2008) states that the drought of 2005 in the south of Brazil may have caused lower river levels northern regions, but there is no clear evidence or quantification of it in literature (Marengo et al. 2008). On the other hand, in general terms and from the sample time series analyzed, there is no evident contrast in the pRI series between the noise present in year 2010 and the noise present in other years of the historic or monitoring period. The noise level

seems relatively constant and stable throughout all the period, in particular throughout the monitoring.

Such observations cannot, however, discard the possible disturbing effect that external climatic disturbances can have in the pRI time series presented, and that has been acknowledged before (Lhermitte et al. 2010). Nevertheless, it is difficult to determine which climatic events may have contributed to the noise of the pRI at each moment and to which extent. We argue here that the noise in NDVI time series from Landsat over tropical areas is too important, and may be hiding the presence of climatic disturbances in the pRI data, especially during the monitoring period. Reducing the level of noise is likely to have a major effect on the distinguishability of deforestation patterns in the pRI time series by BFASTmonitor, and hence a positive effect on the detection accuracy.

The results of this study highlight the importance of removing noise in Landsat NDVI over tropical areas for detection of deforestation. They emphasize as well the need of removing noise from pRI time series, which translates into optimizing the existing noise-removal methods (Lhermitte et al. 2011) and developing new ones if necessary.

The criterion used to define pixels as forested in our study area masked out the majority of the pixels, leaving for the analysis a small part. This is a criterion based on the classes and probabilities of the VCF and FCC layers. This can explain the fact that the optimal window size was the smallest tested (of 7x7), because the forest patches present were of relatively reduced size. Despite the fact that the VCF and FCC layers have a very low Root Mean Square Error, their accuracy does not reach 100% (Sexton et al., 2013), so it is important to acknowledge possible mistakes in the pixels analyzed when interpreting the validation results.

This study is not performed in near real time because the analysis was too computationally extensive for the timeframe available. For the same reason it did not measure the time delay of the detection. However, the validation procedure allowed estimating in general and qualitative terms the temporal performance of BFASTmonitor and compare it after the spatial context had been included. A general decrease in the temporal accuracy was apparent, explained by the presence of noise discussed above.Validation depended on the visual interpretation of Landsat surface reflectance imagery. This implies the validation may be

subjective to a certain level. Also, without having ground truth data or satellite imagery of a higher spatial resolution, the validation may have produced artificially high commission and omission errors (e.g. validation samples in the border between a deforested patch and a forest). Besides, having satellite imagery with higher temporal resolution or from sensors which are not affected by clouds could have made meaningful an assessment of the temporal delay in the detection.

This study relies on the NDVI as an indicator of vegetation dynamics. However, there is evidence in literature that this index may not reflect properly the different stages of regrowth in tropical areas, because young regenerating forests present higher NDVI values than mature ones (Shimabukuro et al., 1998). Also, several studies highlight the limitations of the NDVI in tropical areas, due to its saturation at moderate to high biomass levels (Huete 1997; Phompila et al. 2014; Viña 2012; Wang et al. 2005). Even though saturation was not an issue in the work presented here, several studies signal the advantages of other vegetation indices (Darmawan & Sofan 2014; Huete 1997; Viña 2012). For example, the Enhanced Vegetation Index has been shown to be detect abrupt changes in tropical peat swamp areas with BFAST in a more accurate way than NDVI (Darmawan & Sofan 2014). However further efforts in this direction could determine which vegetation index is most appropriate for tropical evergreen forests (Foody et al. 2003).

Further efforts are needed to determine if the following topics can contribute to increase the accuracy of the detection of deforestation in the tropics from Landsat data with BFASTmonitor. The use of shorter temporal threshold values may clarify if the temporal threshold value represents a significant improvement in the accuracy of the results.
Besides that, the use of single sensors is preferred compared to the fusion of several sensors, due to its simplicity (De Sy et al., 2012). However, recent efforts demonstrated that the fusion of Landsat NDVI and PALSAR time series can improve the accuracy of the detection when compared to that of single sensor systems, also in cases with a high amount of missing data due to persistent cloudiness (Reiche et al., 2015). However authors signal that further research is needed to assess the behavior of the fusion approach under different change scenarios, and that the near real time fusion capabilities must still be addressed (Reiche et al., 2015).

The calibration of the spatial context analysis requires a sensitivity analysis to be carried out for each site (Lhermitte et al. 2010). Veraverbeke et al. (2010) signal that the pRI procedure could be improved by adapting the settings of the control pixel selection to the distance from the focal pixel to the perimeter of the affected patch. It could also be improved by enhancing the performance of the selection in areas where the unchanged pixels belong to highly heterogeneous land cover types (where the procedure is expected to fail to select similar pixels for small window sizes with accuracy). They recognize the difficulty of those recommendations, but acknowledge that the selection procedure could be further improved in that way (Veraverbeke et al. 2010).

The change detection analysis including the spatial context should be made more efficient computationally, so that it can be tested and eventually implemented in near real time. Reiche et al. (2015) recommend adapting the monitoring framework by using BFAST instead of BFASTmonitor if the monitoring period in the tests exceeds 2.75 years, because BFAST is able to detect multiple changes while BFASTmonitor can deal only with single events (Reiche et al., 2015).Validation can be improved by incorporating ground data or by using the TimeSync tool presented by Cohen et al. (2010), that allows to compare the results from change detection algorithms with that of users. Ultimately, an integrated approach that combines remote sensing-based and ground-based monitoring methods is necessary to enhance the capabilities to monitor deforestation in near real-time (DeVries et al., 2013).

7- Conclusion

This study aimed to correct for the effect of outliers and of external disturbances and test whether it improved the detection of BFASTmonitor. Outliers could be distinguished from deforestation events with a temporal threshold shorter than a year (104 days). However, it is not clear whether the removal of remaining outliers improved the detection of deforestation. A slight improvement was observed, which may have been due to the normal variation of the validation samples collected. The spatial neighborhood information could not be used to

correct effectively for the effect of external disturbances, notably during the monitoring period, due to the high level of noise present in the data.

The results highlight the importance of pre-processing the time series used as input for monitoring approaches such as BFASTmonitor. The use of NDVI imagery with remnant outliers after applying Fmask produces acceptable results, that can however be optimized. Theoretically the use of input time series where the effect of external disturbances is corrected for (as with the pRI approach) should help in this direction, but the use of Landsat data for the calculation of the pRI remains complicated due to their irregularity and to cloud contamination. Few approaches have been proposed to reduce noise from time series such as the pRI ones (Lhermitte et al. 2011), and further efforts are needed to test such approaches or develop new ones, and ultimately be able to use a spatial context analysis to improve the detection of deforestation in the tropics.

References

Achard, F., DeFries, R., Eva, H., Hansen, M., Mayaux, P., & Stibig, H.-J. (2007). Pan-tropical monitoring of deforestation. *Environmental Research Letters*, *2*(4), 045022. doi:10.1088/1748-9326/2/4/045022

Ackerman, S. A., Strabala, K. I., Menzel, W. P., Frey, R. A., Moeller, C. C., & Gumley, L. E. (1998). Discriminating clear sky from clouds with MODIS. *Journal of Geophysical Research*, *103*(D24), 32141. doi:10.1029/1998JD200032

Asner, G. P. (2001). Cloud cover in Landsat observations of the Brazilian Amazon. *International Journal of Remote Sensing*, *22*(18), 3855–3862. doi:10.1080/01431160010006926

Asner, G. P., Keller, M., Pereira, Jr, R., Zweede, J. C., & Silva, J. N. M. (2001). Canopy damage and recovery after selective logging in Amazonia: field and satellite studies. *Ecological Applications*, *14*(sp4), 280–298. doi:10.1890/01-6019

Bai, J., & Perron, P. (2003). Computation and analysis of multiple structural change models. *Journal of Applied Econometrics*, *18*(1), 1–22. doi:10.1002/jae.659

Bradley, B. a., Jacob, R. W., Hermance, J. F., & Mustard, J. F. (2007). A curve fitting procedure to derive inter-annual phenologies from time series of noisy satellite NDVI data. *Remote Sensing of Environment*, *106*(2), 137–145. doi:10.1016/j.rse.2006.08.002

Brooks, E. B., Thomas, V. A., Wynne, R. H., & Coulston, J. W. (2012). Fitting the Multitemporal Curve: A Fourier Series Approach to the Missing Data Problem in Remote Sensing Analysis. *IEEE Transactions on Geoscience and Remote Sensing*, *50*(9), 3340–3353. doi:10.1109/TGRS.2012.2183137

Cannon, C. H. (1998). Tree Species Diversity in Commercially Logged Bornean Rainforest. *Science*, *281*(5381), 1366–1368. doi:10.1126/science.281.5381.1366

Chazdon, R. L. (2003). Tropical forest recovery: legacies of human impact and natural disturbances. *Perspectives in Plant Ecology, Evolution and Systematics*, *6*(1-2), 51–71. doi:10.1078/1433-8319-00042

Cohen, W. B., Yang, Z., & Kennedy, R. (2010). Detecting trends in forest disturbance and recovery using yearly Landsat time series: 2. TimeSync — Tools for calibration and validation. *Remote Sensing of Environment*, *114*(12), 2911–2924. doi:10.1016/j.rse.2010.07.010

Coppin, P., Jonckheere, I., Nackaerts, K., Muys, B., & Lambin, E. (2004). Review ArticleDigital change detection methods in ecosystem monitoring: a review. *International Journal of Remote Sensing*, *25*(9), 1565–1596. doi:10.1080/0143116031000101675

Cox, P. M., Betts, R. A., Jones, C. D., Spall, S. A., & Totterdell, I. J. (2000). Acceleration of global warming due to carbon-cycle feedbacks in a coupled climate model. *Nature*, *408*(6809), 184–7. doi:10.1038/35041539

Darmawan, Y., & Sofan, P. (2014, November 4). Comparison of the vegetation indices to detect the tropical rain forest changes using Breaks For Additive Seasonal and Trend (BFAST) Model. *International Journal of Remote Sensing and Earth Sciences (IJReSES)*. Retrieved from http://jurnal.lapan.go.id/index.php/ijreses/article/view/1823

De Sy, V., Achard, F., Asner, G. P., Held, A., Kellndorfer, J., & Verbesselt, J. (2012). Synergies of multiple remote sensing data sources for REDD+ monitoring. *Current Opinion in Environmental Sustainability*, *4*(6), 696–706. Retrieved from http://www.sciencedirect.com/science/article/pii/S1877343512001200

Defries, R., Achard, F., Brown, S., Herold, M., Murdiyarso, D., Schlamadinger, B., & Souza, de. (2007). Earth observations for estimating greenhouse gas emissions from deforestation in developing countries. *Environmental Science & Policy*, *10*(4). Retrieved from http://www.citeulike.org/group/5744/article/2916490

DeFries, R., Asner, G., Achard, F., Justice, C., Laporte, N., Price, K., … Townshend, J. (2005). Monitoring tropical deforestation from emerging carbon markets. Retrieved from http://www.terrabrasilis.org.br/ecotecadigital/pdf/tropical-deforestation-and-climate-change.pdf#page=35

DeFries, R. S., Houghton, R. A., Hansen, M. C., Field, C. B., Skole, D., & Townshend, J. (2002). Carbon emissions from tropical deforestation and regrowth based on satellite observations for the 1980s and 1990s. *Proceedings of the National Academy of Sciences of the United States of America*, *99*(22), 14256–61. doi:10.1073/pnas.182560099

DeVries, B., Pratihast, A. K., Verbesselt, J., Kooistra, L., de Bruin, S., & Herold, M. (2013). Near real-time tropical forest disturbance monitoring using Landsat time series and local expert monitoring data. In *MultiTemp 2013: 7th International Workshop on the Analysis of Multi-temporal Remote Sensing Images* (pp. 1–4). IEEE. doi:10.1109/Multi-Temp.2013.6866022

Diaz-Delgado, R., Salvador, R., & Pons, X. (1998). Monitoring of plant community regeneration after fire by remote sensing. *Fire Management and Landscape Ecology (L. Traboud, editor), International Association of Wildland Fire, Fairfield, Washington*. Retrieved November 26, 2014, from http://www.ebd.csic.es/ricardo/publi/Diaz-Delgado_etal_1998.pdf

Feng, M., Huang, C., Channan, S., Vermote, E. F., Masek, J. G., & Townshend, J. R. (2012). Quality assessment of Landsat surface reflectance products using MODIS data. *Computers & Geosciences*, *38*(1), 9–22. Retrieved from http://www.sciencedirect.com/science/article/pii/S0098300411001439

Foody, G. M., Boyd, D. S., & Cutler, M. E. J. (2003). Predictive relations of tropical forest biomass from Landsat TM data and their transferability between regions. *Remote Sensing of Environment*, *85*(4), 463–474. doi:10.1016/S0034-4257(03)00039-7

Gao, B.-C., Goetz, A. F. H., & Wiscombe, W. J. (1993). Cirrus cloud detection from Airborne Imaging Spectrometer data using the 1.38 μm water vapor band. *Geophysical Research Letters*, *20*(4), 301–304. doi:10.1029/93GL00106

Geerken, R. A. (2009). An algorithm to classify and monitor seasonal variations in vegetation phenologies and their inter-annual change. *ISPRS Journal of Photogrammetry and Remote Sensing*, *64*(4), 422–431. doi:10.1016/j.isprsjprs.2009.03.001

Gibbs, H. K., Brown, S., Niles, J. O., & Foley, J. A. (2007). Monitoring and estimating tropical forest carbon stocks: making REDD a reality. *Environmental Research Letters*, *2*(4), 045023. doi:10.1088/1748-9326/2/4/045023

Global Land Cover Facility (GLCF)and Goddard Space Flight Center (GSFC). 2014. GLCF Forest Cover Change 2000 2005, Global Land Cover Facility,University of Maryland, College Park

Goetz, S. J., Baccini, A., Laporte, N. T., Johns, T., Walker, W., Kellndorfer, J., … Sun, M. (2009). Mapping and monitoring carbon stocks with satellite observations: a comparison of methods. *Carbon Balance and Management*, *4*(1), 2. doi:10.1186/1750-0680-4-2

Goodwin, N. R., Collett, L. J., Denham, R. J., Flood, N., & Tindall, D. (2013). Cloud and cloud shadow screening across Queensland, Australia: An automated method for Landsat TM/ETM+ time series. *Remote Sensing of Environment*, *134*, 50–65. doi:10.1016/j.rse.2013.02.019

Gu, J., Fan, D., Jiang, N., & Liu, J. (2012). A noise detection method for NDVI time series data based on dixon test. In *2012 First International Conference on Agro- Geoinformatics (Agro-Geoinformatics)* (pp. 1–5). IEEE. doi:10.1109/Agro-Geoinformatics.2012.6311708

Gu, J., Li, X., Huang, C., & Okin, G. S. (2009). A simplified data assimilation method for reconstructing time-series MODIS NDVI data. *Advances in Space Research*, *44*(4), 501–509. doi:10.1016/j.asr.2009.05.009

Hagolle, O., Huc, M., Pascual, D. V., & Dedieu, G. (2010). A multi-temporal method for cloud detection, applied to FORMOSAT-2, VENμS, LANDSAT and SENTINEL-2 images. *Remote Sensing of Environment*, *114*(8), 1747–1755. doi:10.1016/j.rse.2010.03.002

Hansen, M. C., Roy, D. P., Lindquist, E., Adusei, B., Justice, C. O., & Altstatt, A. (2008). A method for integrating MODIS and Landsat data for systematic monitoring of forest cover and change in the Congo Basin. *Remote Sensing of Environment*, *112*(5), 2495–2513. Retrieved from http://www.sciencedirect.com/science/article/pii/S0034425707004774

Herold, M., & Johns, T. (2007). Linking requirements with capabilities for deforestation monitoring in the context of the UNFCCC-REDD process. *Environmental Research Letters*, *2*(4), 045025. doi:10.1088/1748-9326/2/4/045025

Herold, M., & Skutsch, M. (2011). Monitoring, reporting and verification for national REDD + programmes: two proposals. *Environmental Research Letters*, *6*(1), 014002. doi:10.1088/1748-9326/6/1/014002

Hilker, T., Wulder, M. A., Coops, N. C., Linke, J., McDermid, G., Masek, J. G., … White, J. C. (2009). A new data fusion model for high spatial- and temporal-resolution mapping of forest disturbance based on Landsat and MODIS. *Remote Sensing of Environment*, *113*(8), 1613–1627. Retrieved from http://www.sciencedirect.com/science/article/pii/S003442570900087X

Holloway, V., & Giandomenico, E. (2009). FCP: The History of REDD Policy. Retrieved October 07, 2014, from http://www.forestcarbonportal.com/resource/history-redd-policy

Houghton, R. A. (1991). Tropical deforestation and atmospheric carbon dioxide. *Climatic Change*, *19*(1-2), 99–118. doi:10.1007/BF00142217

House, J. I., Colin Prentice, I., & Le Quere, C. (2002). Maximum impacts of future reforestation or deforestation on atmospheric CO2. *Global Change Biology*, *8*(11), 1047–1052. doi:10.1046/j.1365-2486.2002.00536.x

Huang, C., Goward, S. N., Masek, J. G., Thomas, N., Zhu, Z., & Vogelmann, J. E. (2010). An automated approach for reconstructing recent forest disturbance history using dense Landsat time series stacks. *Remote Sensing of Environment*, *114*(1), 183–198. doi:10.1016/j.rse.2009.08.017

Huete, A. (1997). A comparison of vegetation indices over a global set of TM images for EOS-MODIS. *Remote Sensing of Environment*, *59*(3), 440–451. doi:10.1016/S0034-4257(96)00112-5

Hyman, R. C., Reilly, J. M., Babiker, M. H., Masin, A. De, & Jacoby, H. D. (2002). Modeling non-CO 2 greenhouse gas abatement, 175–186.

Irish, R. R., Barker, J. L., Goward, S. N., & Arvidson, T. (2006). Characterization of the Landsat-7 ETM Automated Cloud-Cover Assessment (ACCA) Algorithm. Retrieved June 12, 2014, from http://info.asprs.org/publications/pers/2006journal/october/2006_oct_1179-1188.pdf

Jiang, L., Kogan, F. N., Guo, W., Tarpley, J. D., Mitchell, K. E., Ek, M. B., … Ramsay, B. H. (2010). Real-time weekly global green vegetation fraction derived from advanced very high resolution radiometer-based NOAA operational global vegetation index (GVI) system. *Journal of Geophysical Research*, *115*(D11), D11114. doi:10.1029/2009JD013204

Jin, S., & Sader, S. A. (2005). MODIS time-series imagery for forest disturbance detection and quantification of patch size effects. *Remote Sensing of Environment*, *99*(4), 462–470. Retrieved from http://www.sciencedirect.com/science/article/pii/S003442570500307X

Justice, C. ., Townshend, J. R. ., Vermote, E. ., Masuoka, E., Wolfe, R. ., Saleous, N., … Morisette, J. . (2002). An overview of MODIS Land data processing and product status. *Remote Sensing of Environment*, *83*(1-2), 3–15. doi:10.1016/S0034-4257(02)00084-6

Kennedy, R. E., Cohen, W. B., & Schroeder, T. a. (2007). Trajectory-based change detection for automated characterization of forest disturbance dynamics. *Remote Sensing of Environment*, *110*(3), 370–386. doi:10.1016/j.rse.2007.03.010

Kennedy, R. E., Yang, Z., & Cohen, W. B. (2010). Detecting trends in forest disturbance and recovery using yearly Landsat time series: 1. LandTrendr — Temporal segmentation algorithms. *Remote Sensing of Environment*, *114*(12), 2897–2910. doi:10.1016/j.rse.2010.07.008

Lhermitte, S., Verbesselt, J., Verstraeren, W. W., & Coppin, P. (2010). A Pixel Based Regeneration Index using Time Series Similarity and Spatial Context - Photogrammetric Engineering & Remote Sensing - Volume 76, Number 6 / June 2010 - American Society for Photogrammetry and Remote Sensing. *Photogrametric Engineering*. Retrieved from http://essential.metapress.com/content/w4g2m7636k28j112/?genre=article&id=doi:10.14358/PERS.76.6.673

Lhermitte, S., Verbesselt, J., Verstraeten, W. W., Veraverbeke, S., & Coppin, P. (2011). Assessing intra-annual vegetation regrowth after fire using the pixel based regeneration index. *ISPRS Journal of Photogrammetry and Remote Sensing*, *66*(1), 17–27. doi:10.1016/j.isprsjprs.2010.08.004

Li, M., Qu, J. J., & Xianjun, H. (2008). Detecting vegetation change with satellite remote sensing over 2007 Georgia wildfire regions. *Journal of Applied Remote Sensing*, *2*(1), 021505. doi:10.1117/1.2973659

Li, W., Fu, R., Juárez, R. I. N., & Fernandes, K. (2008). Observed change of the standardized precipitation index, its potential cause and implications to future climate change in the Amazon region. *Philosophical Transactions of the Royal Society of London. Series B, Biological Sciences*, *363*(1498), 1767–72. doi:10.1098/rstb.2007.0022

Lyapustin, A., Wang, Y., & Frey, R. (2008). An automatic cloud mask algorithm based on time series of MODIS measurements. *Journal of Geophysical Research*, *113*(D16), D16207. doi:10.1029/2007JD009641

Malhi, Y., Aragão, L. E. O. C., Galbraith, D., Huntingford, C., Fisher, R., Zelazowski, P., … Meir, P. (2009). Exploring the likelihood and mechanism of a climate-change-induced dieback of the Amazon rainforest.

Proceedings of the National Academy of Sciences of the United States of America, *106*(49), 20610–5. doi:10.1073/pnas.0804619106

Marengo, J. A., Nobre, C. A., Tomasella, J., Oyama, M. D., Oliveira, G. S. de, Oliveira, R. de, … Brown, I. F. (2008). The Drought of Amazonia in 2005. Retrieved from http://journals.ametsoc.org/doi/abs/10.1175/2007JCLI1600.1

Marengo, J. A., Tomasella, J., Alves, L. M., Soares, W. R., & Rodriguez, D. A. (2011). The drought of 2010 in the context of historical droughts in the Amazon region. *Geophysical Research Letters*, *38*(12), n/a–n/a. doi:10.1029/2011GL047436

Masek, J. G., Vermote, E. F., Saleous, N. E., Wolfe, R., Hall, F. G., Huemmrich, K. F., … Lim, T.-K. (2006). A Landsat Surface Reflectance Dataset for North America, 1990–2000. *IEEE Geoscience and Remote Sensing Letters*, *3*(1), 68–72. doi:10.1109/LGRS.2005.857030

McKee, T. B., Doesken, N. J., & Kleist, J. (1993). The relationship of drought frequency and duration to time scales. *Eight Conference of Applied Climatology, Anaheim, California*. Retrieved October 03, 2014, from http://ccc.atmos.colostate.edu/relationshipofdroughtfrequency.pdf

Michishita, R., Jin, Z., Chen, J., & Xu, B. (2014). Empirical comparison of noise reduction techniques for NDVI time-series based on a new measure. *ISPRS Journal of Photogrammetry and Remote Sensing*, *91*, 17–28. doi:10.1016/j.isprsjprs.2014.01.003

Morton, D. C., DeFries, R. S., Shimabukuro, Y. E., Anderson, L. O., Arai, E., del Bon Espirito-Santo, F., … Morisette, J. (2006). Cropland expansion changes deforestation dynamics in the southern Brazilian Amazon. *Proceedings of the National Academy of Sciences of the United States of America*, *103*(39), 14637–41. doi:10.1073/pnas.0606377103

Nelson, B. W. (1994). Natural forest disturbance and change in the Brazilian Amazon. *Remote Sensing Reviews*, *10*(1-3), 105–125. doi:10.1080/02757259409532239

Nepstad, D. C., Tohver, I. M., Ray, D., Moutinho, P., & Cardinot, G. (2007). MORTALITY OF LARGE TREES AND LIANAS FOLLOWING EXPERIMENTAL DROUGHT IN AN AMAZON FOREST. *Ecology*, *88*(9), 2259–2269. doi:10.1890/06-1046.1

Olander, L. P., Gibbs, H. K., Steininger, M., Swenson, J. J., & Murray, B. C. (2008). Reference scenarios for deforestation and forest degradation in support of REDD: a review of data and methods. Retrieved from http://iopscience.iop.org/1748-9326/3/2/025011/pdf/1748-9326_3_2_025011.pdf

Oreopoulos, L., Wilson, M. J., & Várnai, T. (2011). Implementation on Landsat Data of a Simple Cloud-Mask Algorithm Developed for MODIS Land Bands. *IEEE Geoscience and Remote Sensing Letters*, *8*(4), 597–601. doi:10.1109/LGRS.2010.2095409

Pereira, R., Zweede, J., Asner, G. P., & Keller, M. (2002). Forest canopy damage and recovery in reduced-impact and conventional selective logging in eastern Para, Brazil. *Forest Ecology and Management*, *168*(1-3), 77–89. doi:10.1016/S0378-1127(01)00732-0

Pesaran, M. H., & Timmermann, A. (2002). Market timing and return prediction under model instability. *Journal of Empirical Finance*, *9*(5), 495–510. doi:10.1016/S0927-5398(02)00007-5

Phelps, J., Webb, E. L., & Agrawal, A. (2010). Land use. Does REDD+ threaten to recentralize forest governance? *Science (New York, N.Y.)*, *328*(5976), 312–3. doi:10.1126/science.1187774

Phillips, O. L., Aragao, L. E. O. C., Lewis, S. L., Fisher, J., Lloyd, J., Lopez-Gonzales, G., … Torres-Lezama, A. (2009). Drought Sensitivity of the Amazon Rainforest. Retrieved from http://agris.fao.org/agris-search/search.do?recordID=FR2014002496

Phompila, C., Lewis, M., Clarke, K., & Ostendorf, B. (2014). Monitoring expansion of plantations in Lao tropical forests using Landsat time series. In T. J. Jackson, J. M. Chen, P. Gong, & S. Liang (Eds.), *SPIE Asia Pacific Remote Sensing* (p. 92601M). International Society for Optics and Photonics. doi:10.1117/12.2068283

Pinard, M., Howlett, B., & Davidson, D. (1996). Site conditions limit pioneer tree recruitment after logging of dipterocarp forests in Sabah, Malaysia. *Biotropica 28(1)*. Retrieved October 03, 2014, from http://www.jstor.org/discover/10.2307/2388766?uid=3738296&uid=2&uid=4&sid=21104269497861

Poulter, B., & Cramer, W. (2009). Satellite remote sensing of tropical forest canopies and their seasonal dynamics. *International Journal of Remote Sensing*, *30*(24), 6575–6590. doi:10.1080/01431160903242005

Powell, S. L., Cohen, W. B., Healey, S. P., Kennedy, R. E., Moisen, G. G., Pierce, K. B., & Ohmann, J. L. (2010). Quantification of live aboveground forest biomass dynamics with Landsat time-series and field inventory data: A comparison of empirical modeling approaches. *Remote Sensing of Environment*, *114*(5), 1053–1068. Retrieved from http://www.sciencedirect.com/science/article/pii/S0034425709003745

R Development Core Team (2011). R: A language and environment for statistical computing. Austria: R Foundation for Statistical Computing Vienna.

Reiche, J., Verbesselt, J., Hoekman, D., & Herold, M. (2015). Fusing Landsat and SAR time series to detect deforestation in the tropics. *Remote Sensing of Environment*, *156*, 276–293. doi:10.1016/j.rse.2014.10.001

Reuter, M., Fischer, J., & Ulbrich, U. (2005). Identification of cloudy and clear sky areas in MSG SEVIRI images by analyzing spectral and temporal information. *Freie Universität, Berlin*. Retrieved from http://www.diss.fu-berlin.de/diss/receive/FUDISS_thesis_000000001661

Román-cuesta, R. M. (uNITED nations F. and A. O. P. (FAO). (2010). Frequently asked questions on REDD+. Retrieved October 07, 2014, from http://www.reddccadgiz.org/documentos/doc_554772732.pdf

Romijn, E., Herold, M., Kooistra, L., Murdiyarso, D., & Verchot, L. (2012). Assessing capacities of non-Annex I countries for national forest monitoring in the context of REDD+. *Environmental Science & Policy*, *19-20*, 33–48. doi:10.1016/j.envsci.2012.01.005

Sano, E. E., Ferreira, L. G., Asner, G. P., & Steinke, E. T. (2007). Spatial and temporal probabilities of obtaining cloud-free Landsat images over the Brazilian tropical savanna. *International Journal of Remote Sensing*, *28*(12), 2739–2752. doi:10.1080/01431160600981517

Saunders, R. W., & Kriebel, K. T. (1988). An improved method for detecting clear sky and cloudy radiances from AVHRR data. *International Journal of Remote Sensing*, *9*(1), 123–150. doi:10.1080/01431168808954841

Schroeder, T. A., Wulder, M. A., Healey, S. P., & Moisen, G. G. (2011). Mapping wildfire and clearcut harvest disturbances in boreal forests with Landsat time series data. *Remote Sensing of Environment*, *115*(6), 1421–1433. Retrieved from http://www.sciencedirect.com/science/article/pii/S0034425711000447

Schultz, M., Verbesselt, J., Herold, M., & Avitabile, V. (2013). Assessing error sources for Landsat time series analysis for tropical test sites in Viet Nam and Ethiopia. In U. Michel, D. L. Civco, K. Schulz, M. Ehlers, & K. G. Nikolakopoulos (Eds.), *SPIE Remote Sensing* (p. 88930M). International Society for Optics and Photonics. doi:10.1117/12.2029374

Sexton, J. O., Song, X.-P., Feng, M., Noojipady, P., Anand, A., Huang, C., … Townshend, J. R. (2013). Global, 30-m resolution continuous fields of tree cover: Landsat-based rescaling of MODIS vegetation continuous fields with lidar-based estimates of error. *International Journal of Digital Earth*, *6*(5), 427–448. doi:10.1080/17538947.2013.786146

Shimabukuro, Y. E., Batista, G. T., Mello, E. M. K., Moreira, J. C., & Duarte, V. (1998). Using shade fraction image segmentation to evaluate deforestation in Landsat Thematic Mapper images of the Amazon Region. *International Journal of Remote Sensing*, *19*(3), 535–541. doi:10.1080/014311698216152

Souza, P. J. de O. P. de, Ribeiro, A., Rocha, E. J. P. da, Farias, J. R. B., Loureiro, R. S., Bispo, C. C., & Sampaio, L. (2009). Solar radiation use efficiency by soybean under field conditions in the Amazon region. *Pesquisa Agropecuária Brasileira*, *44*(10), 1211–1218. doi:10.1590/S0100-204X2009001000001

Townshend, J. R. ., & Justice, C. O. (2002). Towards operational monitoring of terrestrial systems by moderate-resolution remote sensing. *Remote Sensing of Environment*, *83*(1), 351–359. Retrieved from http://www.sciencedirect.com/science/article/pii/S0034425702000822

Tropical Rain Forest Information Center, T. (1998). Rain Forest Report Card: Deforestation of Tropical Rain Forests. Retrieved October 18, 2014, from http://www.trfic.msu.edu/rfrc/status.html

Tucker, C. J., & Townshend, J. R. G. (2000). Strategies for monitoring tropical deforestation using satellite data. *International Journal of Remote Sensing*, *21*(6-7), 1461–1471. doi:10.1080/014311600210263

Uhl, C., & Vieira, I. C. G. (1989). Ecological impacts of selective logging in the Brazilian Amazon: a case study from the Paragominas region of the State of Pará. *Biotropica*, *21*(2), 98–106. Retrieved from http://cat.inist.fr/?aModele=afficheN&cpsidt=19408970

UNEP-GEAS. (2010). Environmental Hotspot Alert. Retrieved October 03, 2014, from http://na.unep.net/geas/hotspots/pdfs/GEAS December.pdf

Veraverbeke, S., Gitas, I., Katagis, T., Polychronaki, A., Somers, B., & Goossens, R. (2012). Assessing post-fire vegetation recovery using red–near infrared vegetation indices: Accounting for background and vegetation variability. *ISPRS Journal of Photogrammetry and Remote Sensing*, *68*, 28–39. doi:10.1016/j.isprsjprs.2011.12.007

Veraverbeke, S., Lhermitte, S., Verstraeten, W. W., & Goossens, R. (2010). The temporal dimension of differenced Normalized Burn Ratio (dNBR) fire/burn severity studies: The case of the large 2007 Peloponnese wildfires in Greece. *Remote Sensing of Environment*, *114*(11), 2548–2563. doi:10.1016/j.rse.2010.05.029

Veraverbeke, S., Lhermitte, S., Verstraeten, W. W., & Goossens, R. (2011). A time-integrated MODIS burn severity assessment using the multi-temporal differenced normalized burn ratio (dNBRMT). *International Journal of Applied Earth Observation and Geoinformation*, *13*(1), 52–58. doi:10.1016/j.jag.2010.06.006

Verbesselt, J., Hyndman, R., Newnham, G., & Culvenor, D. (2010). Detecting trend and seasonal changes in satellite image time series. *Remote Sensing of Environment*, *114*(1), 106–115. Retrieved from http://www.sciencedirect.com/science/article/pii/S003442570900265X

Verbesselt, J., Hyndman, R., Zeileis, A., & Culvenor, D. (2010). Phenological change detection while accounting for abrupt and gradual trends in satellite image time series. *Remote Sensing of Environment*, *114*(12), 2970–2980. doi:10.1016/j.rse.2010.08.003

Verbesselt, J., Zeileis, a, & Herold, M. (2012). Near real-time disturbance detection using satellite image time series. *Remote Sensing of Environment*, *123*(Turner 2010), 98–108. doi:10.1016/j.rse.2012.02.022

Verbesselt, J., Zeileis, A., & Herold, M. (2012). Near real-time disturbance detection using satellite image time series. *Remote Sensing of Environment*, *123*, 98–108. doi:10.1016/j.rse.2012.02.022

Verdin, J., Funk, C., Senay, G., & Choularton, R. (2005). Climate science and famine early warning. *Philosophical Transactions of the Royal Society of London. Series B, Biological Sciences*, *360*(1463), 2155–68. doi:10.1098/rstb.2005.1754

Viña, A. (2012). Evaluating vegetation indices for assessing productivity along a tropical rain forest chronosequence in Western Amazonia. *Israel Journal of Plant Sciences*, *60*(1), 123–133. doi:10.1560/IJPS.60.1-2.123

Viovy, N., Arino, O., & Belward, A. S. (1992). The Best Index Slope Extraction (BISE): A method for reducing noise in NDVI time-series. *International Journal of Remote Sensing*, *13*(8), 1585–1590. doi:10.1080/01431169208904212

Wang, C., Qi, J., & Cochrane, M. (2005). Assessment of Tropical Forest Degradation with Canopy Fractional Cover from Landsat ETM+ and IKONOS Imagery. Retrieved from http://journals.ametsoc.org/doi/abs/10.1175/EI133.1

White, M. a., & Nemani, R. R. (2006). Real-time monitoring and short-term forecasting of land surface phenology. *Remote Sensing of Environment*, *104*(1), 43–49. doi:10.1016/j.rse.2006.04.014

WWF. (2013). Deforestation rates in Brazil surge, after years of progress to slow forest loss. Retrieved October 03, 2014, from http://wwf.panda.org/what_we_do/footprint/forestry/?212402/Deforestation-rates-in-Brazil-surge-after-years-of-progress-to-slow-forest-loss

Xin, Q., Olofsson, P., Zhu, Z., Tan, B., & Woodcock, C. E. (2013). Toward near real-time monitoring of forest disturbance by fusion of MODIS and Landsat data. *Remote Sensing of Environment*, *135*, 234–247. Retrieved from http://www.sciencedirect.com/science/article/pii/S0034425713001235

Zeng, N., Yoon, J.-H., Marengo, J. A., Subramaniam, A., Nobre, C. A., Mariotti, A., & Neelin, J. D. (2008). Causes and impacts of the 2005 Amazon drought. *Environmental Research Letters*, *3*(1), 014002. doi:10.1088/1748-9326/3/1/014002

Zhu, Z., & Woodcock, C. E. (2012). Object-based cloud and cloud shadow detection in Landsat imagery. *Remote Sensing of Environment*, *118*, 83–94. Retrieved from http://www.sciencedirect.com/science/article/pii/S0034425711003853

Appendix: amount of observations per pixel

a) Amount of observations before the removal of remnant outliers in the historic period

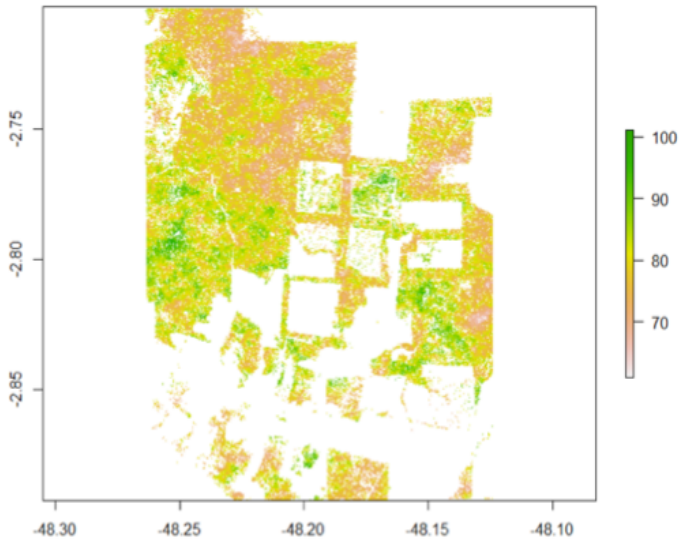

b) Amount of observations after the removal of remnant outliers in the historic period

c) Amount of remaining observations after the removal of remnant outliers in the monitoring period